

MICROCOPY RESOLUTION TEST CHART  
NATIONAL BUREAU OF STANDARDS-1963-A

Copy 1 of 2

②

AD-A171 431

INVESTIGATION OF THE UHF MOBILE-RADIO  
PROPAGATION CHANNEL IN A TEMPERATE-  
ZONE FORESTED ENVIRONMENT

Kenneth J. White, CPT, SC  
HQDA, MILPERCEN (DAPC-OPA-E)  
200 Stovall St.  
Alexandria, VA 22332

DTIC  
SELECTE  
AUG 28 1986  
S D

Final Report, 13 August 1986

DISTRIBUTION STATEMENT A: Approved for public release; distribution  
is unlimited.

DTIC FILE COPY

A thesis submitted to MICHIGAN TECHNOLOGICAL UNIVERSITY, Houghton, MI,  
49931, in partial fulfillment of the requirements for the degree of  
MASTER OF SCIENCE IN ELECTRICAL ENGINEERING.



BLOCK 20 (cont):

vertical and horizontal polarizations. Given an 8.8 km transmission path with the signal penetrating 1.3 km of forest just before reaching the receiver, the ratio of coherent (direct wave) intensity to total received signal power is 42% for horizontal polarization and 5% for vertical polarization. The results of the research indicate that long transmission paths in foliage are better characterized by a "forward-scattering" mechanism than by a lateral wave model.



**INVESTIGATION OF THE UHF MOBILE-RADIO  
PROPAGATION CHANNEL IN A TEMPERATE-ZONE  
FORESTED ENVIRONMENT**

**By**

**KENNETH J. WHITE**

**CAPTAIN, US ARMY SIGNAL CORPS**

**A THESIS**

**Submitted in partial fulfillment of the requirements**

**for the degree of**

**MASTER OF SCIENCE IN ELECTRICAL ENGINEERING**

**MICHIGAN TECHNOLOGICAL UNIVERSITY**

**1986**

This thesis, "Investigation of the UHF Mobile-Radio Propagation Channel in Temperate-Zone Forested Environments" is hereby approved in partial fulfillment of the requirements for the degree of MASTER OF SCIENCE IN ELECTRICAL ENGINEERING.

DEPARTMENT OF ELECTRICAL ENGINEERING

Richard L. Campbell  
Richard L. Campbell, Ph. D  
Thesis Advisor

E. Keith Stanek  
E. Keith Stanek, Ph. D  
Head of Department

Dated 8/13/86



Accession For	
NTIS CRA&I	<input checked="" type="checkbox"/>
DTIC TAB	<input type="checkbox"/>
Unannounced	<input type="checkbox"/>
Justification	
By	
Distribution /	
Availability Codes	
Dist	Avail and/or Special
A-1	

ABSTRACTINVESTIGATION OF THE UHF MOBILE-RADIO PROPAGATION CHANNEL  
IN A TEMPERATE-ZONE FORESTED ENVIRONMENT

by

Kenneth J. White

Experimental verification of the stochastic power-spectral-density theory of radio propagation, as applied to a mobile receiver in a forested environment, is presented. Using a novel technique to achieve fractional-hertz resolution of the diffuse and direct wave components of the Doppler-spread received spectrum, the resultant data taken at 432 MHz shows that the angle of arrival of the diffuse component of the incident energy at the receive antenna is described by an uniform probability density function for both vertical and horizontal polarizations. Given a 8.8 kilometer transmission path with the signal penetrating 1.3 km of forest just before reaching the receiver, the ratio of coherent (direct wave) intensity to total received signal power is 42% for horizontal polarization and 5% for vertical polarization. The excess path loss above free-space-loss is examined and the impact of the results on existing theories of propagation in foliage is discussed.

TABLE OF CONTENTS

<b>Abstract</b>	<b>iii</b>
<b>Acknowledgements</b>	<b>v</b>
<b>Disclaimer of Product Endorsement</b>	<b>vi</b>
<b>List of Tables and Figures</b>	<b>vii</b>
<b>Introduction</b>	<b>1</b>
<b>Field Expressions and Statistics</b>	<b>4</b>
<b>Power-Spectral Theory of Propagation</b>	<b>9</b>
<b>Experimental Apparatus</b>	<b>18</b>
<b>Experiment Environment</b>	<b>27</b>
<b>Processing and Results</b>	<b>31</b>
<b>Discussion and Comparison with Previous Work</b>	<b>44</b>
<b>Conclusions</b>	<b>57</b>
<b>References</b>	<b>61</b>
<b>Appendix A: Derivation of Theoretical Plots</b>	<b>A1</b>
<b>Appendix B: Random-Pairs Method Of Forest Survey</b>	<b>B1</b>
<b>Appendix C: HP 5451C Fourier Analysis</b>	<b>C1</b>
<b>Appendix D: Rayleigh-Effective-Volume Model</b>	<b>D1</b>

ACKNOWLEDGEMENTS

My utmost thanks and appreciation go to Dr. Richard L. Campbell for his unflagging support, unbounded patience, and constant encouragement. This thesis, indeed, could not have been accomplished without him and I will be forever in his debt. I would also like to thank my committee members, Dr. J.A. Soper, Dr. R.E. Zulinski, Dr. C.T. Young, and Dr. Campbell for their generous time and effort and for their excellent contributions to the final report. I must also thank my office-mate, Scott Belanger, for his careful review of the draft and for graciously permitting numerous interruptions of his own studies to allow me to bounce ideas and questions off him as I prepared the thesis. A heart-felt thank-you goes to Professors Soper, Hambley, Wiitanen, and Johnson for their excellent classroom instruction and their ever-generous personal help in assisting me in the successful completion of my studies. I must also express my undying love and gratitude to my wife, Lynn, not only for her continuous support and encouragement, but also for her tireless work as my "field assistant". A big hug and kiss go to "Dooba" and the "Pook-a-pook" for lovingly understanding when their old man couldn't play with them because he was busy "working on the computer again!".

DISCLAIMER OF PRODUCT ENDORSEMENT

The identification of certain commercial products and instruments is to sufficiently document the experimental procedure. In no case does such identification imply recommendation or product endorsement by MICHIGAN TECHNOLOGICAL UNIVERSITY or the US ARMY, nor does it necessarily suggest that the material or equipment identified is the best uniformly available for the stated purpose.

LIST OF TABLES AND FIGURES

<u>TABLES</u>	page
Table 1. Forest Survey Results	30.1
 <u>FIGURES</u>	
1. Experiment Environment	3
2. Experiment Geography	5
3. Arrival Angle of Diffuse Component	11
4a. Theoretical Angular Spectrum, Vertical	16
4b. Theoretical Angular Spectrum, Horizontal	17
4c. Theoretical Angular Spectrum, Urban Study	19
5. Experiment Equipment	20
6. Filter Response	22
7a. Receiver Configuration	24
7b. Roof-mounted Half-wave Dipole Antenna	25
8. Reception-Area Map	28
9. Signal Path Profile	29
10a. Vertical Probe Spectrum	32
10b. Horizontal Probe Spectrum	33
10c. Cross-polarized Probe Spectrum	34
11. Vertical Received Spectrum	37
12. Horizontal Received Spectrum	38
13. Cross-polarized Received Spectrum	39

14.	Vertical Angular Spectrum	41
15.	Horizontal Angular Spectrum	42
16.	Cross-polarized Angular Spectrum	43
17.	Spatial Correlation, Vertical Polarization	45
18.	Spatial Correlation, Horizontal Polarization	46
19.	Urban Environment Co-polarized Angular Spectrum	48
20.	Excess Path Loss Curve	51
21.	Lateral Wave Model	53
B1.	Random-Tree-Pairs Survey Technique	B3
D1.	Rayleigh Effective Volume Propagation Model	D3

## INTRODUCTION

This decade has seen a rapid increase in the military and commercial demand for quality high-capacity mobile communications in both voice and data applications. The new technologies in mobile communications are quickly being embraced by the US Army as the complex dynamics of the modern battlefield and the rigors of the army's new Air-Land Battle doctrine have vastly increased the demand for communications. Additionally, the intense lethality of the latest weapons systems dictates that both the fighting elements and their headquarters be constantly "on the move" [1]. To add greater system flexibility, survivability, and capacity, the army is supplementing its traditional terrestrial-based systems with tactical satellite links for both fixed and mobile subscribers.

Essential to the continued development of quality and reliable mobile communications systems for the battlefield is the formulation and verification of predictive propagation models for the tactical environment. The Air Force Systems Command and the Army's Communications-Electronics Command in recent years have been instrumental in the military effort in the formulation of such models [2] - [9] while Bell Laboratories personnel and others have been

been in the fore-front on the civilian side [10] - [22]. In an attempt to assist in the characterization of a mobile-radio propagation channel through a forested environment (which comprises a dominant portion of the potential battlefield in many of the areas of strategic interest to the United States), this paper presents the results of research based on the stochastic power-spectral theory of propagation [10], [11] utilizing a fine-resolution spectrum analysis technique developed by Campbell [18].

Fig. 1 shows the experimental approach taken in this study. A mobile receiver is constrained to move at constant velocity along a straight stretch of road which has been cut through a homogeneous forested stand. A CW transmitter is placed some miles from the forest and transmits a signal in a direction orthogonal to the road. The receiver will receive energy via the "direct wave" that propagates directly from the transmitter through the forest (ray R1) as well as waves reflected from the ground (R2). These waves combine at the antenna as the "coherent" field. Energy also reaches the receiver from those waves that are scattered from the trees (rays R3 and R4). These latter waves comprise the "incoherent" or "diffuse" field incident at the antenna. An extensive effort has been made in determining the characteristics and behavior of the "coherent" intensity, but little is known about the diffuse

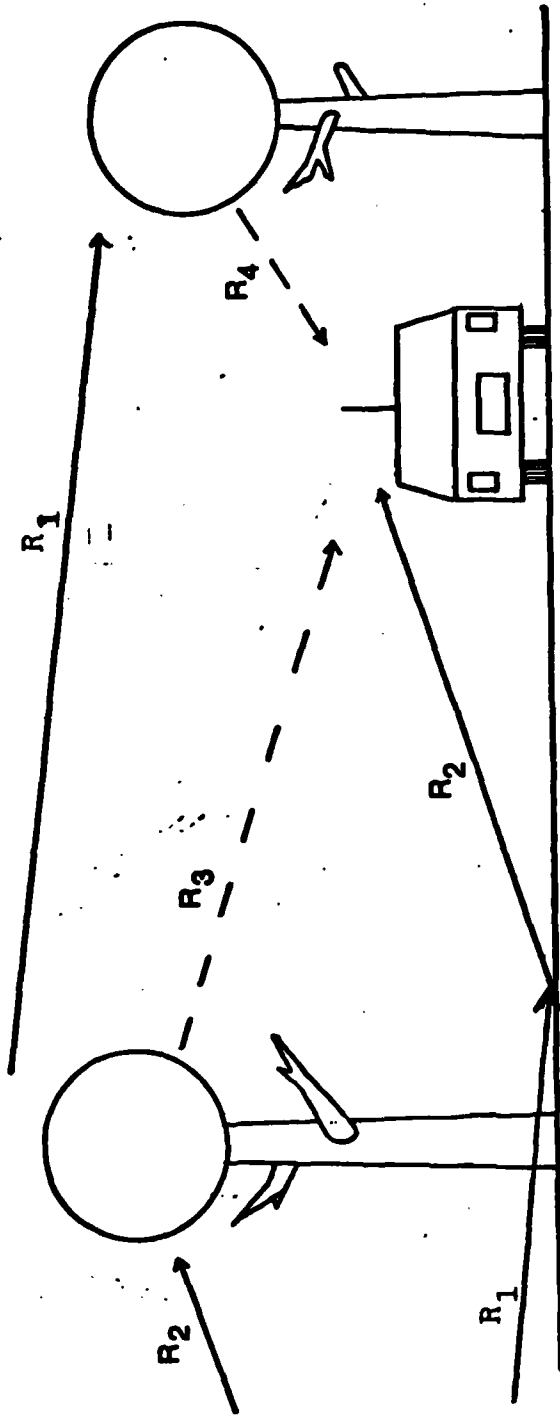


FIGURE 1. EXPERIMENT ENVIRONMENT

component. The nature of the latter is of concern to theorists and designers of both terrestrial and satellite mobile links [23] and will provide insight into the overall propagation mechanism of the medium. This study provides measurements of the coherent and incoherent intensities resulting from a forest propagation path at 432 MHz and examines the power-spectral-density of the received signal. The impact of the experimental results on the existing general theories of propagation through forests will also be discussed.

#### FIELD EXPRESSIONS AND STATISTICS

Fig. 2 shows an aerial view of the mobile receiver traveling at velocity "Vo" through the forested stand with the CW source transmitting normal to the direction of vehicle travel. A portion of the diffuse component scattered from a tree forward of the vehicle arrives at angle "α". The direct wave will be received by the antenna at the transmitter frequency,  $f_c$ , but the incoherent wave will be Doppler shifted to:

$$f(\alpha) = f_c + (V_o / \lambda) \cos \alpha \quad (1)$$

Note that waves scattered from objects forward of the vehicle will be shifted higher in frequency while those

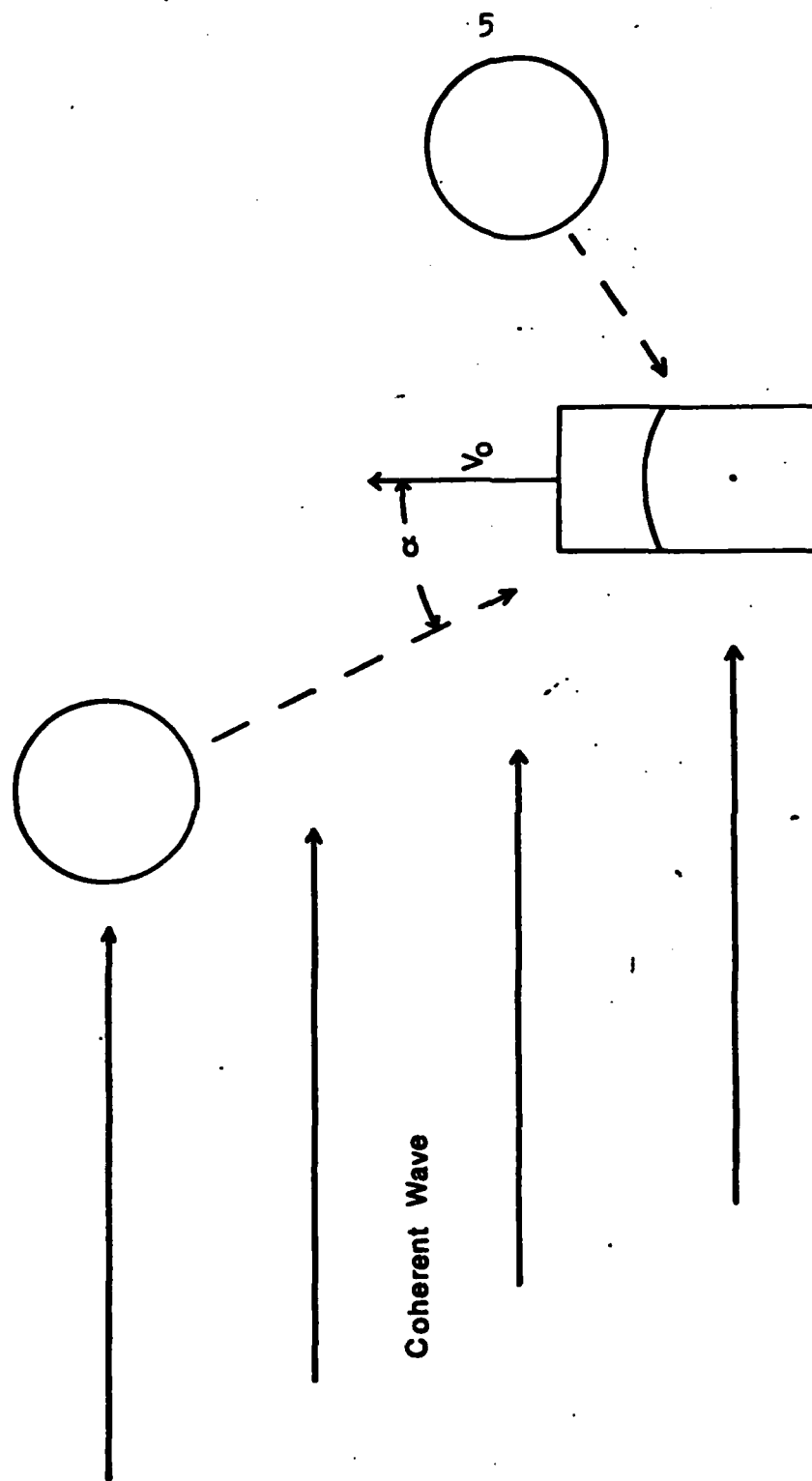


FIGURE 2. EXPERIMENT GEOMETRY

scattered from behind will be shifted down in frequency with a maximum possible shift of  $f_m$ :

$$f_m = V_0/\lambda \quad (2)$$

The bandwidth of the received signal will therefore be 2 times  $f_m$ . For example, with a vehicle velocity of 30 mph and wavelength of 69.4 cm (432 MHz), the bandwidth of the signal at the receiver will be about 39 Hz. It remains then to describe the statistics of the signals comprising this narrow bandwidth.

An electromagnetic field which fluctuates about some mean value, such as the signal from the CW transmitter in this study, can be expressed at some point in space (eg., any point along the vehicle path in fig. 1) as the sum of its mean value (coherent contribution) plus its zero-mean contributions (fluctuating or diffuse component). Using the complex envelope representation of the signal, this may be expressed as:

$$u(r,t) = \langle u(r,t) \rangle + u_f(r,t) \quad (3)$$

Considering the forest to be a random medium of discrete scatterers and following the definitions and notation of Ishimaru [24], the total intensity, then, is the sum of the

coherent and incoherent field intensities:

$$\begin{aligned}
 I_T &= \langle |u(r,t)|^2 \rangle = I_c + I_i & (4) \\
 &= |\langle u(r,t) \rangle|^2 + \langle |u_p(r,t)|^2 \rangle
 \end{aligned}$$

where the brackets indicate an ensemble average and "t" indicates a time dependency. If the medium of propagation consists of fixed random scatterers, then the propagation is at least a wide-sense stationary (and presumably ergodic) process. Ensemble averages are then equivalent to time averages [25] and measurements of the intensity of both components of the signal "u(r)" may be made at a number of points taken sequentially rather than simultaneously. This is the approach used in this study.

By treating the field at any point in the vehicle path as a random variable, the autocorrelation function  $R_{uu}(\tau)$  between the field at any two points separated in time by "τ" is expressed as:

$$\begin{aligned}
 R_{uu}(\tau) &= \langle u(t)u^*(t+\tau) \rangle & (5) \\
 &= \lim_{T \rightarrow \infty} \frac{1}{T} \int_0^T u(\tau) u^*(t+\tau) dt
 \end{aligned}$$

Expanding the integrand and dropping terms which result in zero mean results in:

$$\begin{aligned}
 R_{uu}(\tau) &= |\langle u \rangle|^2 + \langle u_f(t) u_f^*(t + \tau) \rangle \\
 &= I_c + R_f(\tau)
 \end{aligned}
 \tag{6}$$

where:  $R_f(\tau)$  is the autocorrelation of the fluctuating component.

The above autocorrelations are expressed in " $\tau$ " or the separation in time between points being considered. Since this separation is a function of vehicle velocity, the above equations may be expressed as spatial correlations through the relationship:

$$\text{distance } d = V_o * \tau \tag{7}$$

For any random process " $x(t)$ ", the autocorrelation function of " $x(t)$ " when evaluated at " $\tau = 0$ " yields the average power of the process ( $E[X^2(t)]$ ). Thus,  $R_f(0)$  equals the incoherent intensity [25].

As noted above, the power-spectral-density (PSD) of the signal incident at the mobile receiver is a primary factor to be examined in this study. According to the Wiener-Khintchine theorem [25], the PSD of a wide-sense stationary process and its autocorrelation function form a Fourier transform pair. Hence,

$$S(f) = \int_{-\infty}^{\infty} R_{uu}(\tau) \exp(-j2\pi f\tau) d\tau \tag{8}$$

Note that the PSD and the autocorrelation functions are real even functions of "f" and "τ" respectively.

Furthermore, the PSD may be changed from a frequency spectrum to angular spectrum via:

$$f = (V_0/\lambda) * \cos\alpha \quad (9)$$

This latter distinction will assist in interpreting the experimental results to determine the angular contribution of the incoherent field relative to the receiver.

#### POWER-SPECTRAL THEORY OF PROPAGATION

The PSD theory of propagation as presented here was developed in the early 1970s by Bell Laboratories [10] - [12]. It was initially accepted as an accurate model based on the experimental results of Cox [14]-[16]. Further efforts to confirm the theory have been hampered by the very narrow fractional bandwidth ( $2V_0/c$ ;  $c$  - speed of light) of the Doppler-spread signal. Utilizing a novel approach (described below), Campbell [18] was able to obtain millihertz resolution of the received signal and thus demonstrate the validity of the theory and refine it for the urban environment (some of his results are presented here).

In the Bell Labs model, the field at the receiver is modeled

as the summation of a number of horizontally traveling plane waves with random amplitudes, arrival angles and phases (see fig. 3). The phases are uniformly distributed between 0 and  $2\pi$ . The theory initially assumes that the arrival angles are similarly distributed. Given a vertically polarized signal, the average (incoherent) field is characterized:

$$E_z = E_0 \sum_{n=1}^N C_n * \cos(\omega_c t + \omega_n t + \phi_n) \quad (10)$$

where:  $\omega_c$  - transmitted (radial) frequency

$\omega_n$  - doppler shift (radial)

$\phi_n$  - random phase

$C_n$  - normalization constant such that

$$\langle C_n^2 \rangle = 1$$

For large values of  $N$ , the Central Limit Theorem leads to the presumption that the field is a narrow-band Gaussian random process and, hence, a wide-sense stationary process [26]. Following traditional communications theory [27], the field may be further expressed in terms of its in-phase and quadrature components:

$$E_z = T_c(t)\cos(\omega_c t) - T_s(t)\sin(\omega_c t) \quad (11)$$

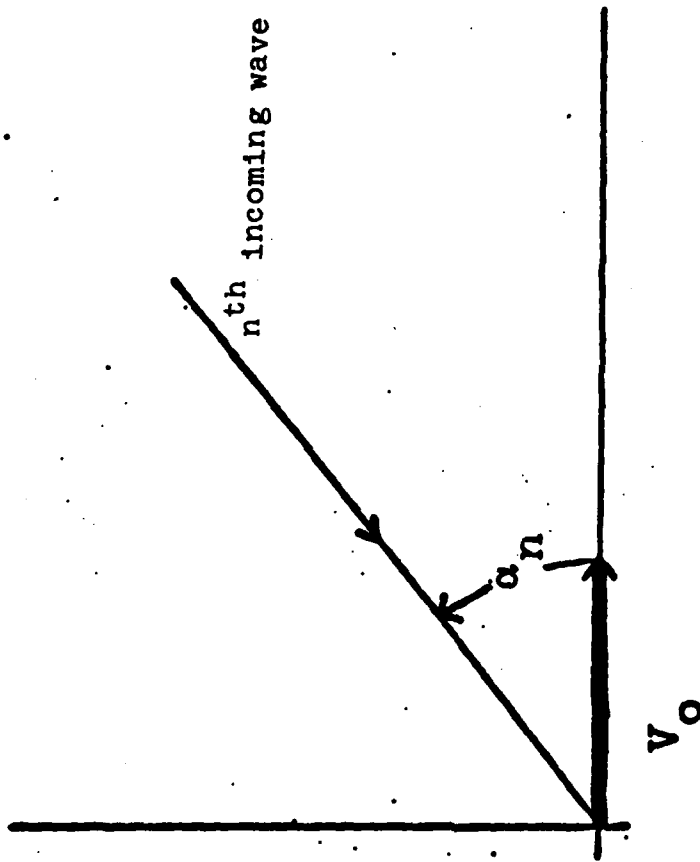


FIGURE 3. ARRIVAL ANGLE OF DIFFUSE COMPONENT

$$T_c(t) = E_0 \sum_n^N C_n * \cos(\omega_n t + \phi_n)$$

$$T_s(t) = E_0 \sum_n^N C_n * \sin(\omega_n t + \phi_n)$$

$T_c(t)$  and  $T_s(t)$  are therefore Gaussian random processes and possess zero mean and equal variance:

$$\langle T_c^2 \rangle = \langle T_s^2 \rangle = \frac{E_0^2}{2} = \langle |E_z|^2 \rangle \quad (12)$$

where  $T_c$  and  $T_s$  signify the random variables corresponding to the quadrature components at fixed "t" and are assumed to be uncorrelated. Note also that the average power is equal to the variance. The envelope of  $E_z(r)$ :

$$r = (T_c^2 + T_s^2)^{\frac{1}{2}} \quad (13)$$

is Rayleigh distributed.

Having established the field expressions and their relevant statistics, it now remains to develop the predictive formulae for the power spectrum. Given a large number of scatterers in the the environment, it is reasonable to assume a continuous distribution of power incident on the antenna within some differential angle. Hence, we can express the differential received power at the mobile antenna with respect to arrival angle as:

$$\int b G(\alpha) p(\alpha) d\alpha \quad (14)$$

where:  $b$  - total average power received by isotropic antenna.

$G(\alpha)$  - directive gain of receiving antenna

$p(\alpha) d\alpha$  - fraction of total incoming power within  $d\alpha$

Recalling the formula for Doppler shift as a function of arrival angle (eq. 1), and noting that  $f(\alpha) = f(-\alpha)$ , the differential variation of power as a function of arrival angle and frequency is:

$$S(f) |df| = b[p(\alpha)G(\alpha) + p(-\alpha)G(-\alpha)] |d\alpha| \quad (15)$$

Since

$$\alpha = \cos^{-1} \frac{(f-f_c)}{f_m} \quad (16)$$

the final expression for the model of the PSD of the received signal at the mobile receiver antenna (ie., the situation as shown in fig. 2) is:

$$S(f) = \frac{b[p(\alpha)G(\alpha) + p(-\alpha)G(-\alpha)]}{[f_m - (f-f_c)^2]^{\frac{1}{2}}} \quad (17)$$

for  $|f - f_c| < f_m$ , otherwise  $S(f) = 0$

This is essentially a two-dimensional model, in that all of the "N" incident waves are assumed to arrive at a near horizontal elevation angle. A more complicated model accounting for a three-dimensional distribution of arriving energy was developed by Aulin [28]. However, the Campbell study [18], as well as the results of the current research, indicate that the simpler model presented above is an adequate representation. Furthermore, measurements by Lee and Brandt [29] show that the angle of arrival of the incoming energy for a mobile receiver in an urban environment is concentrated within 16 degrees of the horizon.

The physical model of eq. (17) accounts for the PSD of the diffuse component of the received energy but does not include the direct wave. The direct wave may be accounted for in the model by adding to eq. (17) the expression below.

$$B G(\alpha_c) \delta(f - f_c - f_0) + S_d(f) \quad (18)$$

where:  $\alpha_c$  - arrival angle of direct wave

$$f_o = f_m * \cos \alpha_c$$

B - magnitude weighting factor

$S_d(f)$  - PSD of amplitude/phase fluctuations of  
the direct wave

Equations (17) and (18) taken together represent the model against which the experimental results obtained in this study will be compared. Note that the addition of the coherent contribution results in a Rician probability function for the signal envelope. A complete discussion of the model to include consideration of cross-correlations, statistical moments, level-crossing rates, fading properties, and coherence bandwidths, is presented in references [10], [11], and [13].

The model may be represented as a frequency spectrum as above, or as an angular spectrum via eq. 16. This spectrum shows the distribution of intensity as a function of arrival angle (fig. 2). As the nature of the scattering environment will manifest itself in the expression for  $p(\alpha)$ , the angular spectrum presentation of the measured intensity gives greater insight into the propagation mechanism. Figs 4a, b show the theoretical normalized plots of the PSD as angular spectrum for the case where there is a uniform distribution of scattered energy incident on the receiver antenna (ie.,

# THEORETICAL ANGULAR SPECTRUM

VERTICAL POLARIZATION

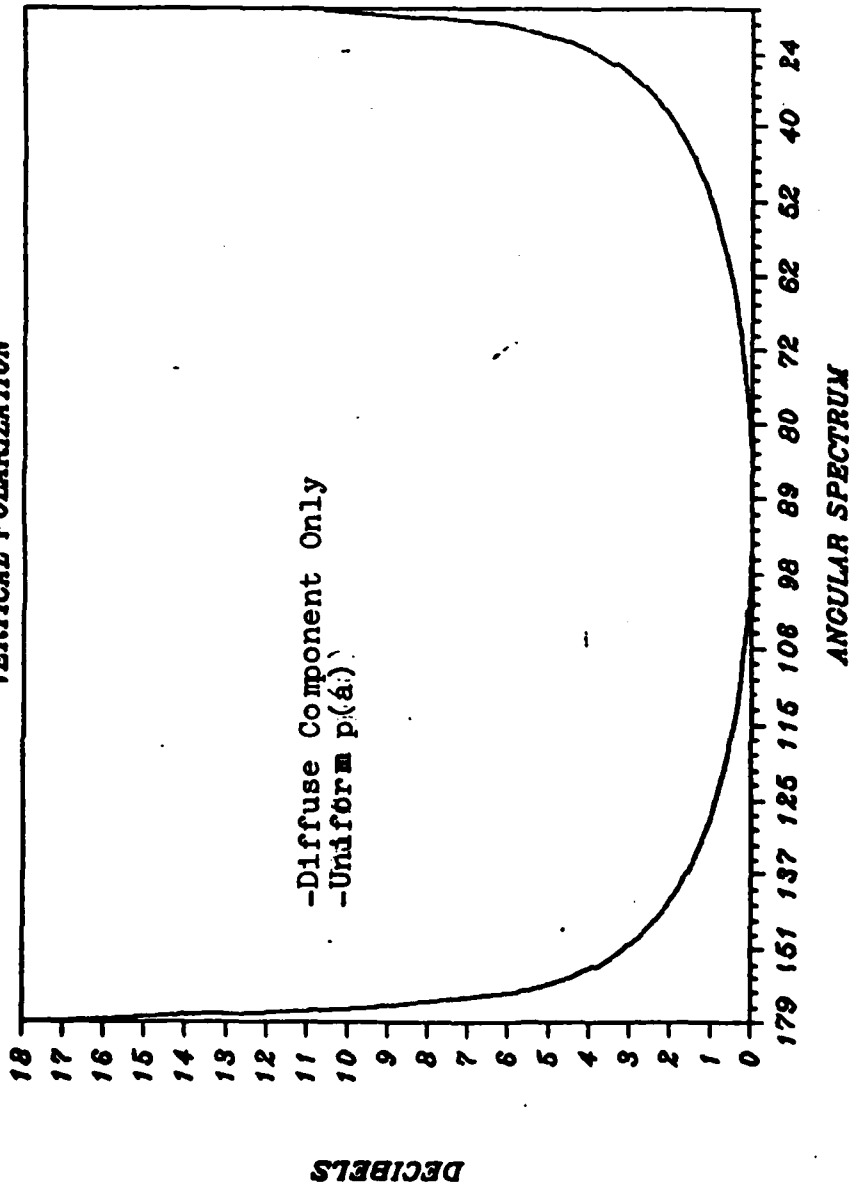


FIGURE 4a

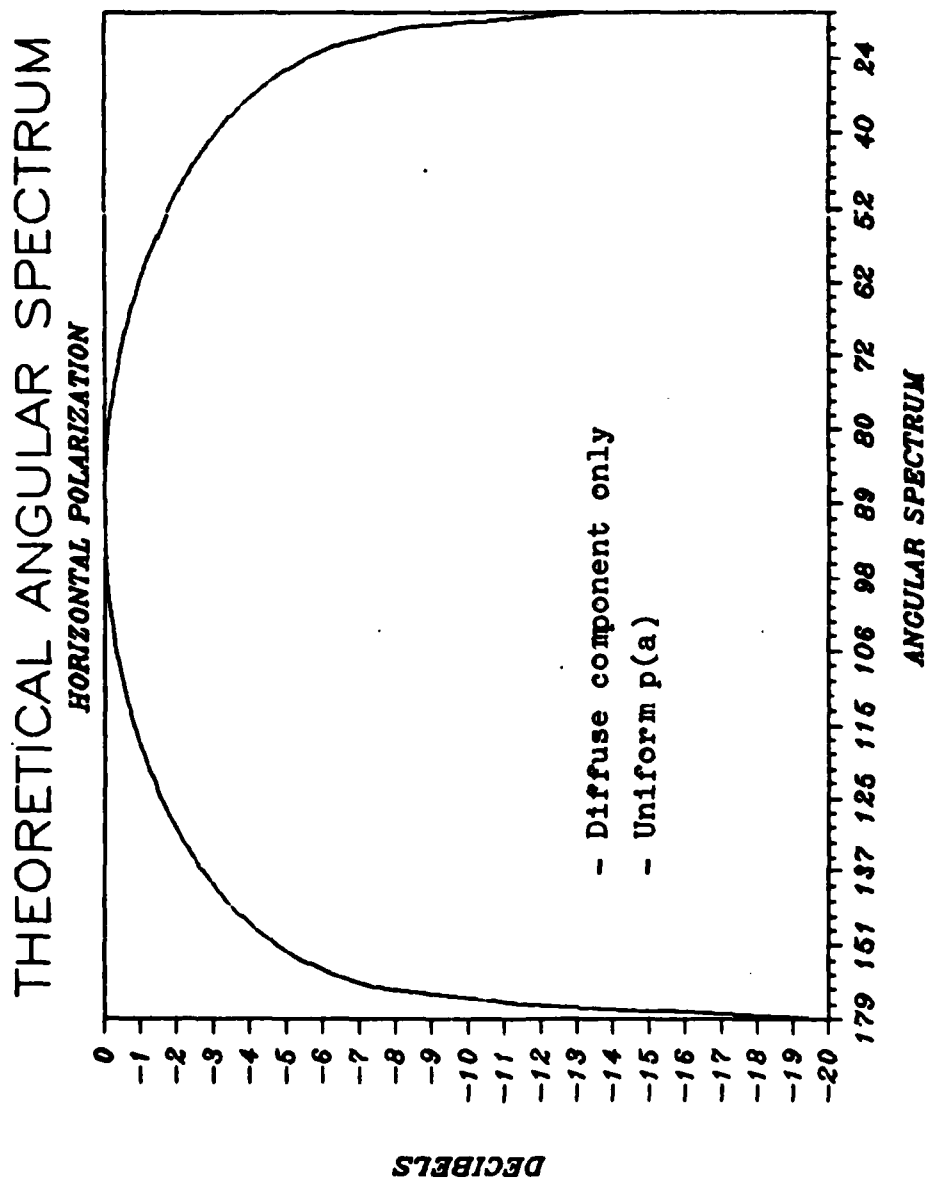


FIGURE 4b

$p(\alpha) = 1/(2\pi)$  for both a vertically-polarized and a horizontally-polarized receiving half-wave dipole antenna (transmitter is copolarized). Campbell [18], in refining the model for the suburban environment, suggested a different  $p(\alpha)$  based on the delay-spread measurements of Cox [15] which showed that scatterers nearest to the moving receiver made the greatest contribution to the received energy. Given the scattering geometry of a vehicle moving down a residential street with buildings on each side, and noting that the power arriving from any one scatterer (building) should be inversely proportional to the square of its distance from the receiver, Campbell [18] suggests that  $p(\alpha) = \sin^2 \alpha / \pi$  for the urban environment. This results in the PSD of fig. 4c.

#### EXPERIMENTAL APPARATUS

In order to acquire meaningful data to verify the above theory, the two most significant problems that had to be overcome in the experimental process were frequency drift in the receiver and transmitter and the lack of an available spectrum analyzer with fractional-hertz resolution at UHF radio frequencies. The technique used in this study was developed by Campbell [18] and used successfully in his propagation studies in the suburban environment. A block diagram of the equipment used is in fig. 5. The very stable

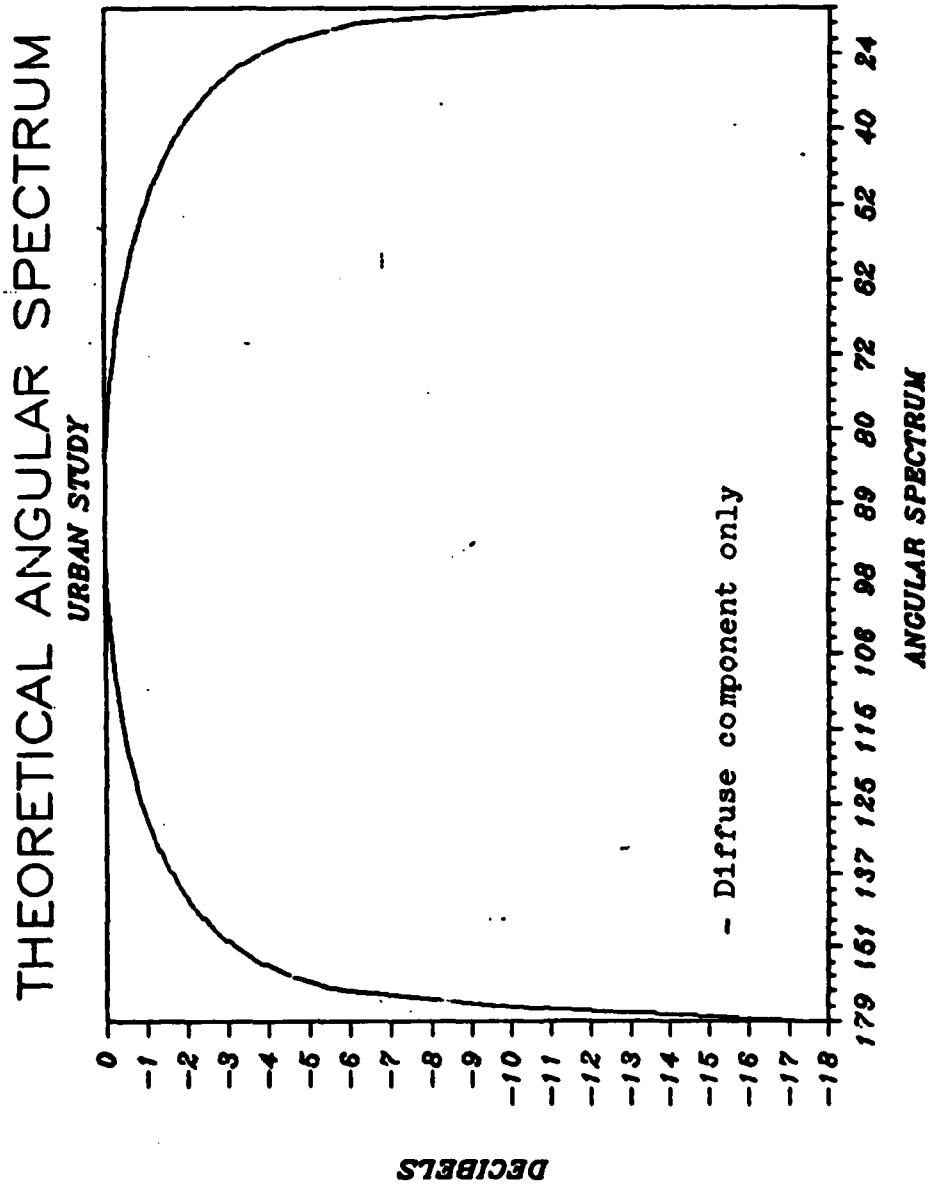


FIGURE 4c

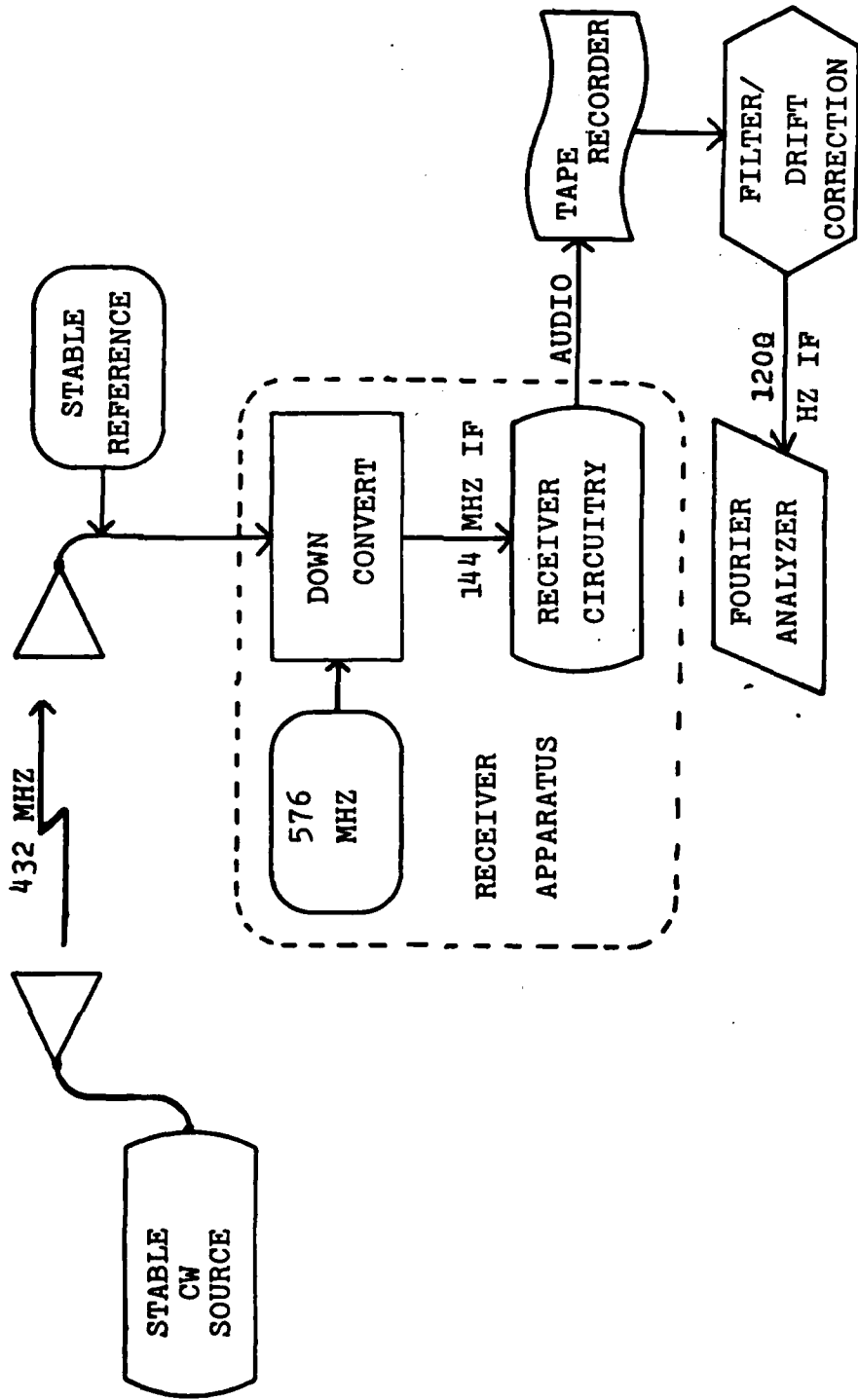


FIGURE 5. EXPERIMENT EQUIPMENT

CW transmitter is set at 432.2 MHz and radiates into an KLM-420-47C-14 antenna (48 degree beamwidth). The receiving antenna is a half-wave dipole with balun. The frequency drift of the transmitter was found to be less than 0.5 Hz over the period that the individual data runs were being conducted. This resolution, although not ideal, is sufficient to discern the pattern of the received PSD.

The next obstacle was the measured receiver drift of  $> 18$  Hz/hour. This was compensated for in the following manner. First the output of a very stable 5 MHz "Vectron" oscillator was divided via TTL logic down to 100 kHz. The resultant pulse has a very high harmonic content into the UHF band. This frequency "comb" is then inserted to one port of a hybrid combiner at the receiver input. The transmitter is tuned to a frequency about 1200 Hz below one of the reference harmonics near 432 MHz. The received signal is then injected into the other port of the combiner. The lower side-band receiver is tuned so that the reference harmonic at the audio output is at about 1800 Hz and the received signal is centered at 600 Hz. While the receiver will cause both the reference and the received signal to vary over the course of a data run, the difference frequency between the two will remain constant at 1200 Hz. By inserting the output of the receiver (either directly or after recording on magnetic tape) into the 8th-order Butterworth filters

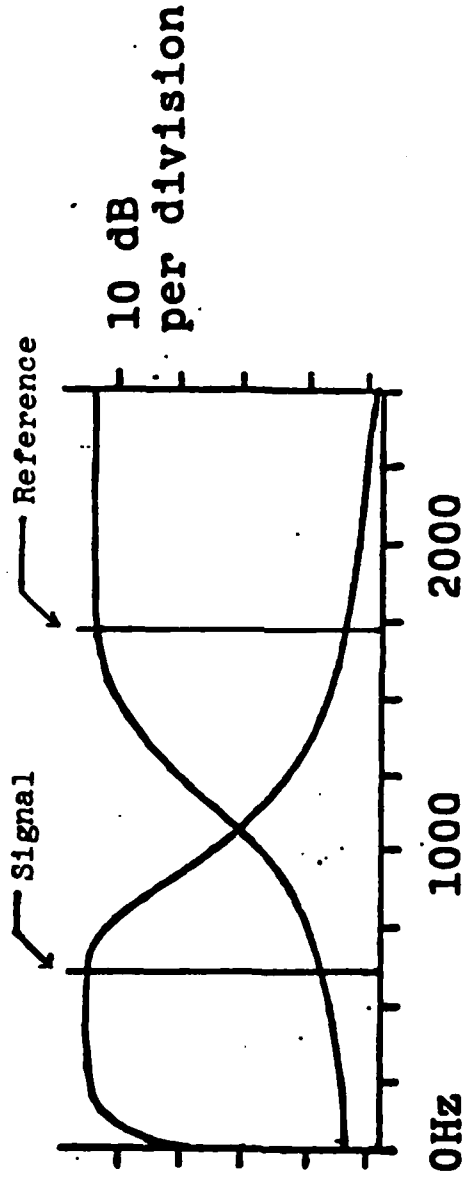


FIGURE 6. FILTER RESPONSE

shown in fig. 6 to separate the reference and the signal, and by applying them respectively to the saturating and non-saturating inputs of an XR-2208 analog multiplier IC, the resultant output is the PSD of the received signal-down-converted and centered on the audio-range difference frequency of about 1200 Hz. While any transmitter drift will still be present in the final signal, the receiver drift will be removed by this mixing process. The specific technique used here was to play the output of the receiver directly into a high-quality "SONY" TC-D5M portable tape-recorder for recording on "MAXELL XL-II" cassettes during the data runs for later processing in the lab.

The actual data gathering was performed in the following manner. Having selected a suitable environment in which to conduct the experiment (see below), the receiver apparatus was mounted in the back-seat of a 1984 Toyota Corolla (fig. 7a). A wooden roof rack was constructed on which to mount the half-wave dipole about 76.2 cm above the roof of the car (in order to mitigate any effects of the auto on the received pattern and to approach having the antenna in as close to a free-space environment as possible). See fig. 7b. The car was then driven to the north end of the selected path. Next, the reference and signal frequencies were aurally compared with a tuning fork to ensure they were at about 1800 and 600 Hz. An identifying signal was then



FIGURE 7a. RECEIVER CONFIGURATION

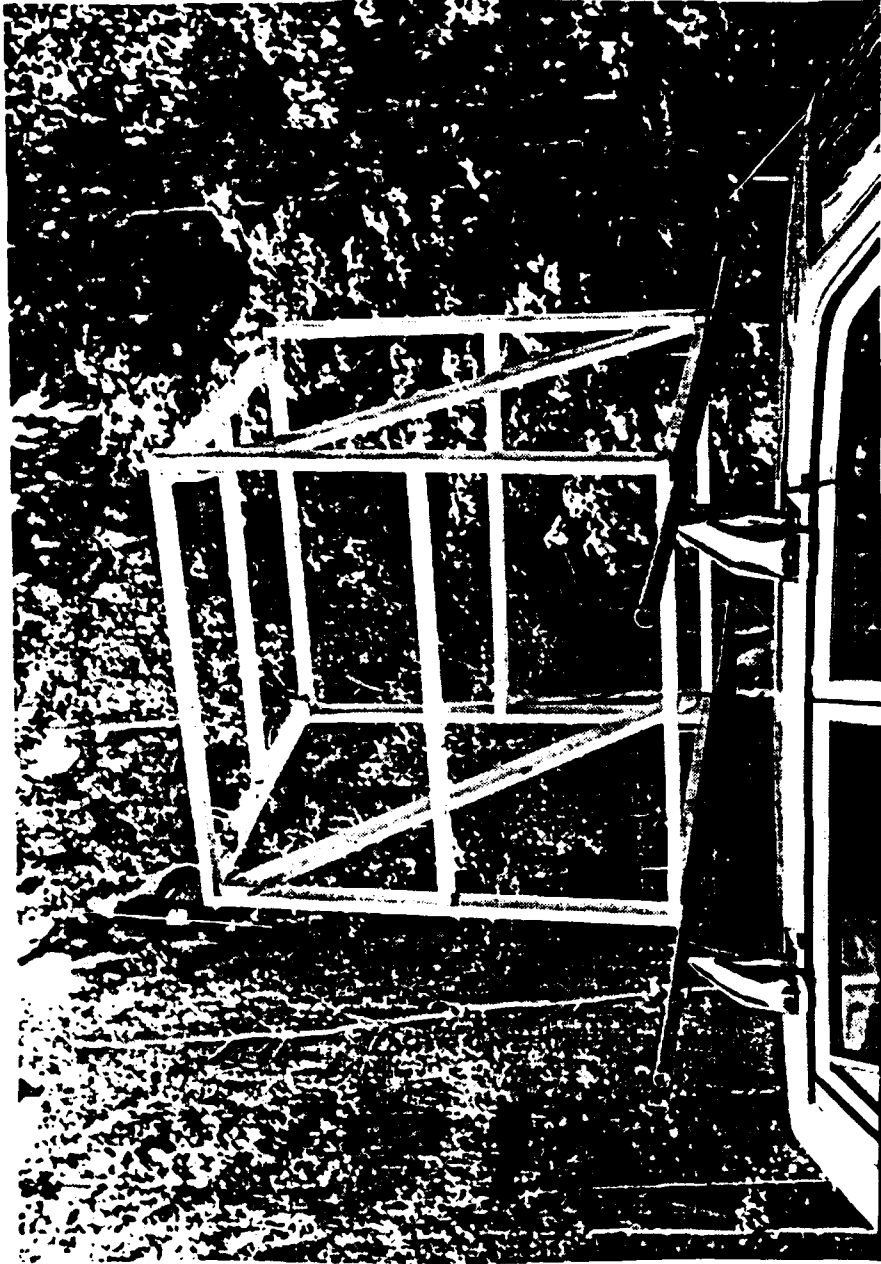


FIGURE 7b; ROOF-MOUNTED HALF-WAVE DIPOLE ANTENNA

placed on the tape by keying the reference on and off with a toggle switch. Following a one-minute wait, the car was accelerated up to a steady 84 kph ( $\pm 0.8$  kph over the entire run). The reference was keyed off/on when the car passed the designated start point of the run. The actual length of the path over which constant velocity data was taken was 1.0 km (vertical/cross-polarized runs) or 1.6 km (horizontal runs). The reference was again keyed off/on at the end of the test path (the start and stop points of the run were marked by easily identifiable terrain features). The car was then slowed to a stop and turned around. The complete procedure was repeated three more times.

The entire experiment was conducted once with both antennas vertically polarized (path length 1.0 kilometers), once horizontally polarized (1.6 km long path), and once with the transmitter vertically polarized and the receiver horizontally polarized (same path as vertical). The data was initially checked for usefulness by playing the tape into the filters/multiplier board whose output was in turn attached to a HP 3582A Spectrum Analyzer. If accepted, the data was played into the HP 5451C Fourier Analyzer for storage and analysis.

## EXPERIMENT ENVIRONMENT

A map of the experiment geography is shown in fig. 8. The area is located on the Keweenaw peninsula in northern Michigan. Data was taken during wind-less days in late May and early June when the trees were in full-leaf. The transmitter antenna was located on top of a residential home about 70 meters from the western shore of Portage Lake. The mobile receiver covered the routes shown in fig. 8. The road was located about 8.8 km from the transmitter. An exaggerated profile chart of the radio link at about the mid-point of the receiver path is shown in fig. 9. The total elevation change over the length of the data runs was about 5 meters. At the receiver, the angle of incidence of the direct wave is less than 0.4 degrees. Based on the profile and the average tree height (see below), the propagating radio wave first encounters the forest about 1.6 km from the receiver. The amount of forest penetrated by the direct wave varies over the route of the mobile receiver from just less than 1.0 km to about 1.6 km (as evidenced by the open areas indicated on the map) and averages about 1.2 km for the vertical/co-polarized data route and 1.4 km for the horizontal route.

The forest was surveyed using the random-tree-pairs sampling

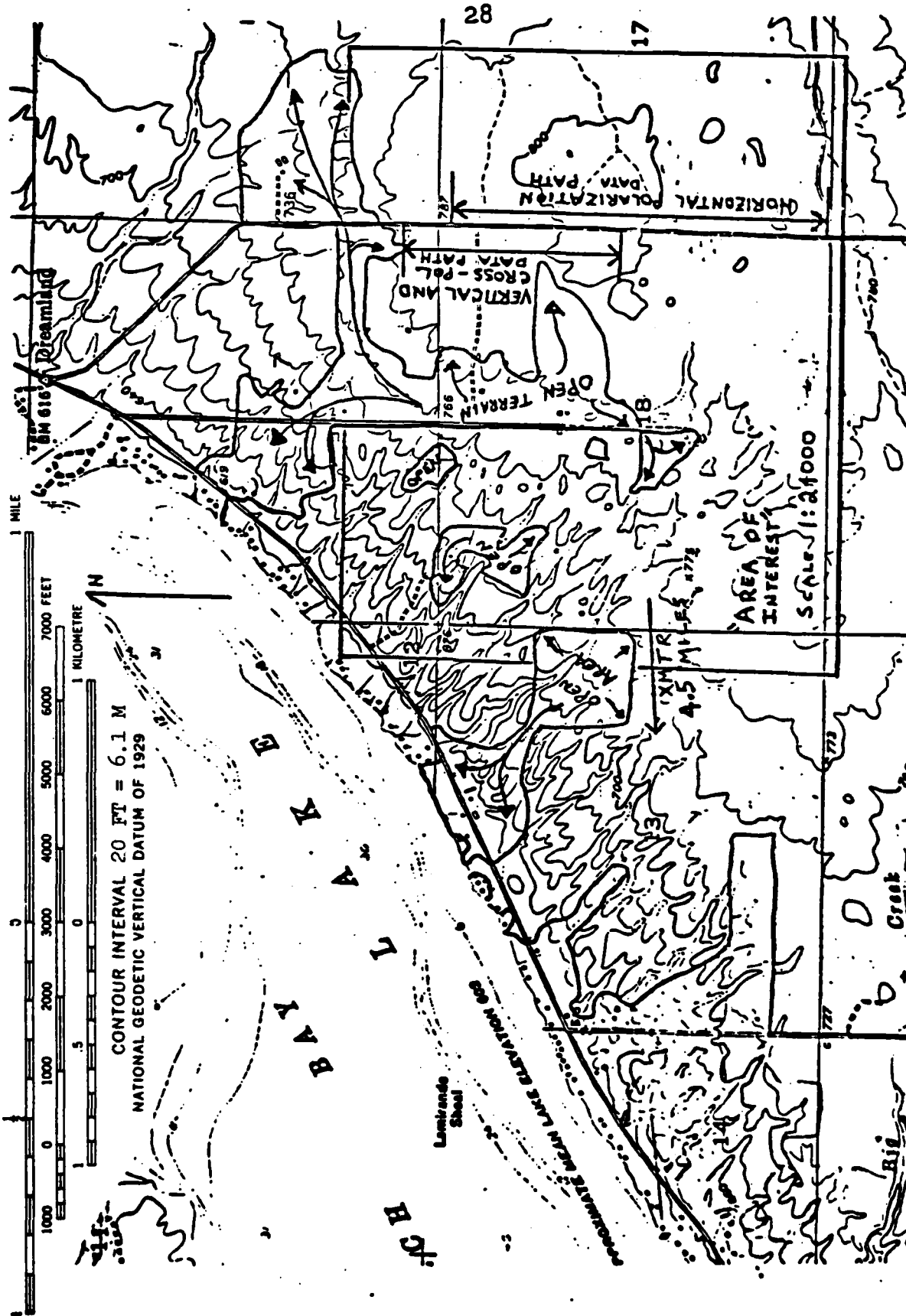
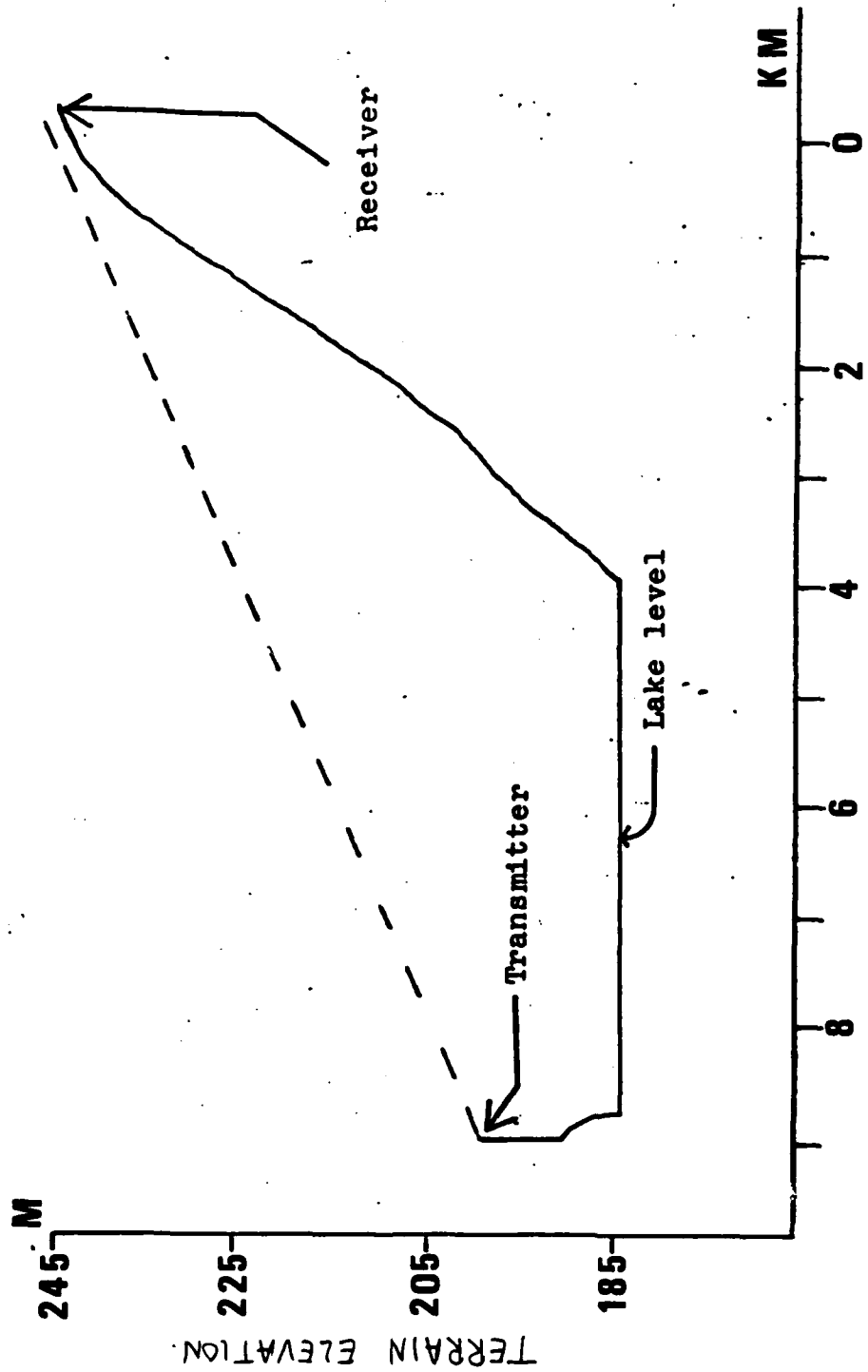


FIGURE 8. RECEPTION-AREA MAP



DISTANCE FROM RECEIVER

FIGURE 9. SIGNAL PATH PROFILE

method [30] - [32] (see Appendix B for a brief description of this technique). This method lends itself well to performing rapid surveys of forested stands and had been utilized by the author in the past. The results of the survey are presented in table 1. In brief, the forest consists predominately of maple trees about 0.7 meters in circumference and 13 meters tall. The coefficient of variation for the tree diameter suggests that this is a medium-aged stand of 60-70 year old trees. There are a large number of "reproduction class" trees (3-10 cm in diam.) throughout the area. A light-to-moderate undergrowth of ferns and grasses is prevalent in the flatter eastern portion of the area-of-interest indicated on the map, while a much thicker and taller undergrowth predominates over the more-sloping western side. The crowns of the deciduous trees extend about 15-30% down the height of the tree and are characterized by an upright wide-mouthed-cone shape on their undersides topped by a hemispherical upper region. The hemlocks take on a "christmas-tree" shape over 75-80% of their height.

The road and the accompanying shoulders and drainage ditches occupy a well-defined 25-meter-wide gap in the forest. The open areas present in the transmission path within 1.6 km of the road are characterized by fern growth 60-80 cm high, with a smattering of young scotch pine, as well as a few

TABLE B1. Forest Survey Results

Species	Average Diameter (cm)	Diam. Std. Dev.	Average Height (m)	Hgt. Std. Dev.	Relative Density (%)
Maple	23.04	9.31	13.64	2.20	82
Birch	24.23	7.47	14.33	3.17	10
Hemlock	34.37	14.46	13.40	2.60	4
Aspen	29.68	9.02	15.00	0.43	3
Others	--	--	--	--	< 1
Mean Area Per Tree (All types)		15.26 square meters			
Trees per Hectare (> 10 cm diam.)		655.14 trees per hectare			
Repro. Class Trees (3-10 cm diam.)		785.46 trees per hectare			

aspen and birch seedlings. The transition zone between the open areas and the main stand of forest is dominated by 7-9 meter tall scotch pines six or more meters apart. The forestation pattern indicated on the map is generally accurate within the area surveyed. Based on the author's brief survey, the pattern of forestation along the transmitted path as it appears to the mobile receiver is essentially a quasi-stationary random process. It should also be noted that the transmitter antenna must radiate its energy through a small stand of about 30-meter-high mixed hardwood trees before encountering open air.

#### PROCESSING AND RESULTS

"Probe" spectra are recordings of the received signal while the car was waiting motionless for one minute prior to accelerating to speed to start the run. These are referred to as "probes" since the received PSD's taken during the data runs are the actual Doppler-spread spectra convolved with the probe. Representative probes for each experiment configuration are shown in fig. 10a - c. The horizontal and vertical co-polarized probes were taken about 0.5 km north of the northern end of the test routes (see fig. 8) while the cross-polarized probe was recorded at a point about 0.5 km south of the southern end of the data route.

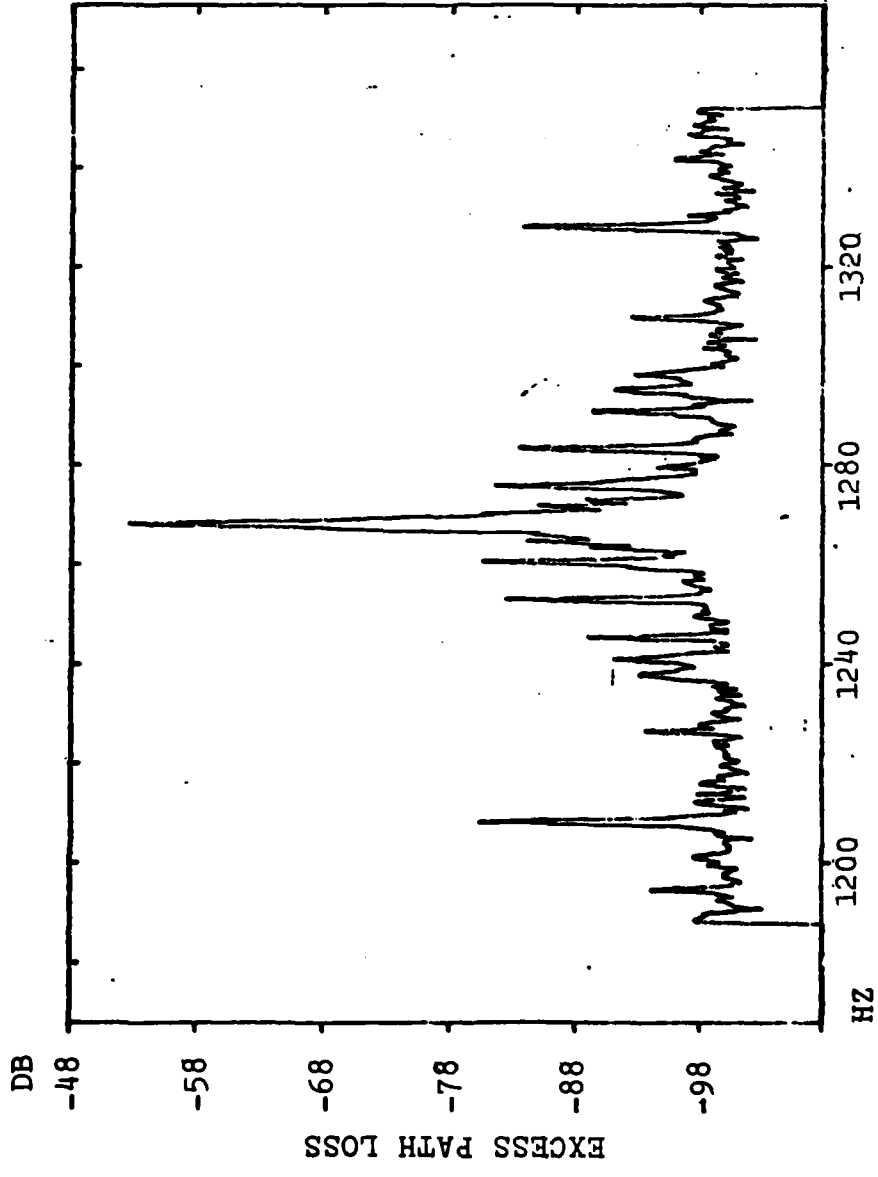


FIGURE 10a. VERTICAL PROBE SPECTRUM

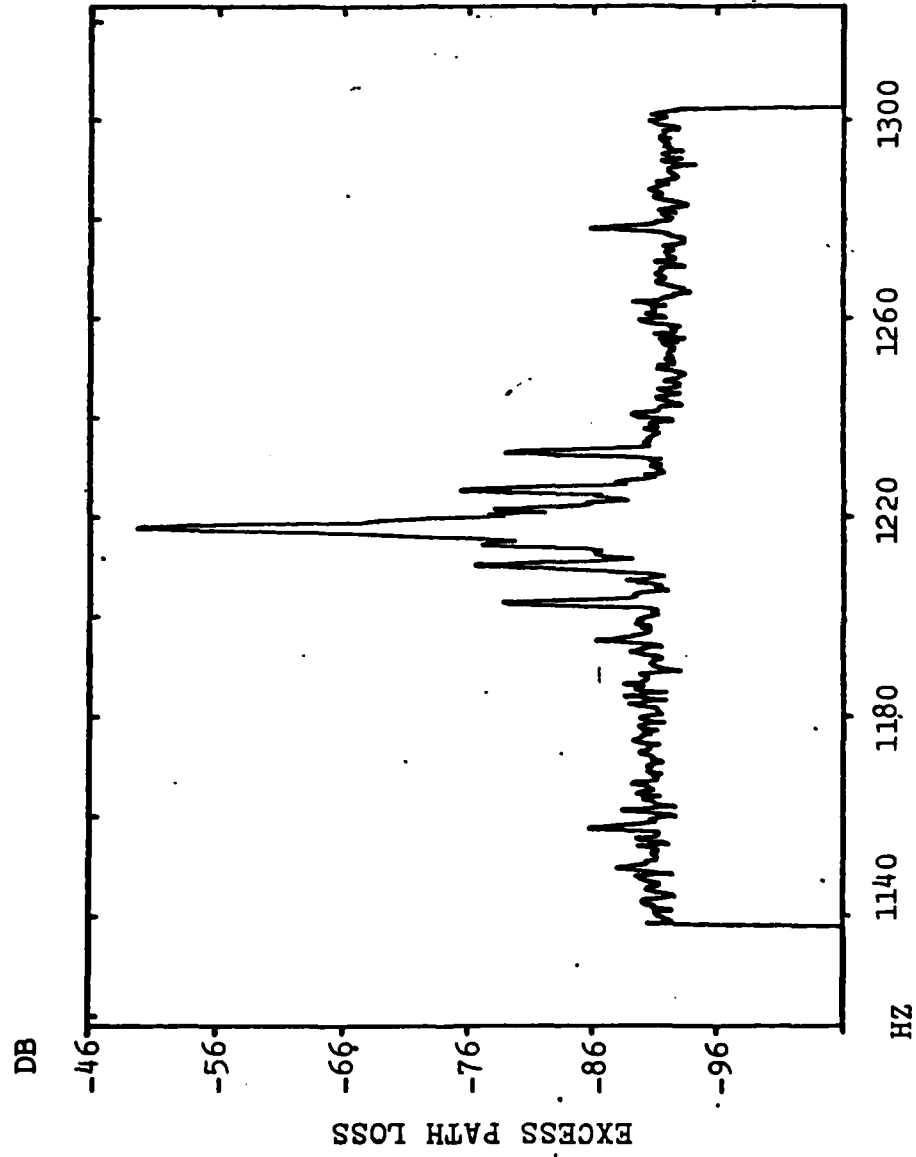


FIGURE 10b. HORIZONTAL PROBE SPECTRUM

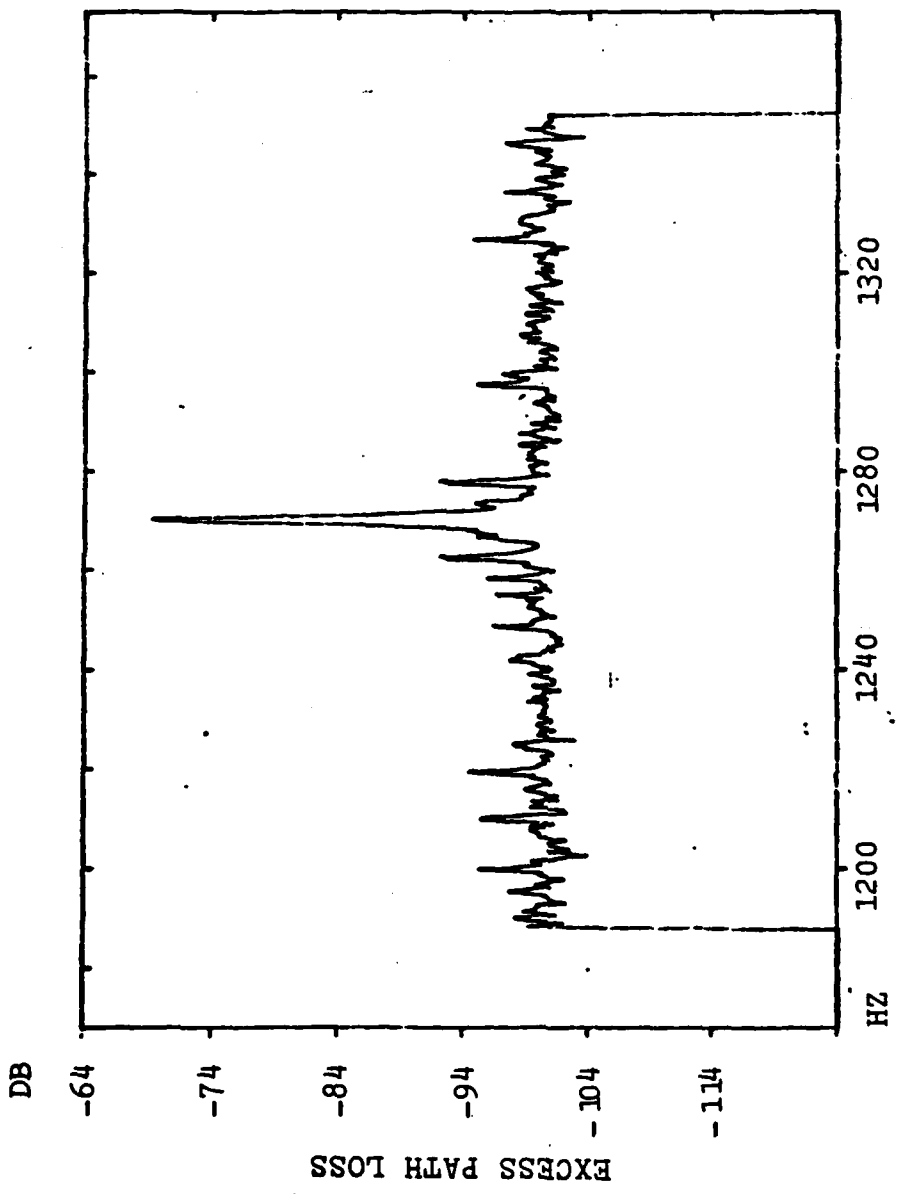


FIGURE 10c. CROSS-POLARIZED PROBE SPECTRUM

The received signal is clearly seen as the main peak in the center of the spectrum almost 30 dB higher than any of the other peaks. The recorder speed fluctuates slightly during the recording and playback process ("wow and flutter"): The results of this fluctuation are easily seen as the sideband peaks in the probe spectrum. While a totally "clean" probe (no sideband peaks) is desired, the probe plots indicate that the sidebands should have little effect on the received data. Furthermore, the lack of a spectral spread around the received signal indicates the static nature of the environment. Transmitter drift can also be ascertained by examining the probes just prior and following a data run.

As noted above, the data was processed using an HP 5451C Fourier Analyzer (see Appendix C for a brief discussion of the procedures used). The narrow bandwidth spectra were obtained by using the "Band-Selectable Fourier Analysis" (BSFA) software package that was supplied with the machine [33] (Bendat and Piersol [34] discuss zoom-transform techniques applicable to BSFA). The resultant spectral resolution is 0.4 Hz per point (channel). The incoming time record was multiplied by a single Hanning window, so the equivalent noise bandwidth of each channel is 0.6 Hz [35]. As noted above, frequency drift is on the order of less than 0.5 Hz so frequency uncertainty within the plots is bounded by +/- 1 channel. The normalized standard error estimate for

the amplitudes presented in the spectral plots is a function of the number of averages and effective bandwidth used in sampling the data [34]. During the processing of the data from each run, the BSPA parameters were adjusted to insure that the entire time record of the run would be averaged over to produce the resultant power spectra. This resulted in 16 averages for the vertically polarized and cross-polarized runs and 22 averages for the horizontally polarized runs and the probe spectra. This yields normalized standard errors for the cross-polarized and vertical spectrums of 0.354 and 0.302 for the probes and horizontal spectrums. The sampling distribution is described by a chi-square distribution with 32 (vertical and cross polarized) or 44 (horizontal and probes) degrees of freedom [34]. This results in a 90% confidence interval for the true PSD of  $[0.68 * \text{MPSD}, 1.6 * \text{MPSD}]$  for the vertical and cross-polarized results ("MPSD" denotes the measured PSD) and an interval  $[0.71 * \text{MPSD}, 1.47 * \text{MPSD}]$  for the horizontal results.

The received and processed power-spectral-densities for each of the three polarization situations are presented in fig. 11 - 13. They represent the single data run out of the four for each polarization over which vehicle speed was the most constant and the least transmitter drift occurred. The Doppler-spread of the diffuse component is easily seen in

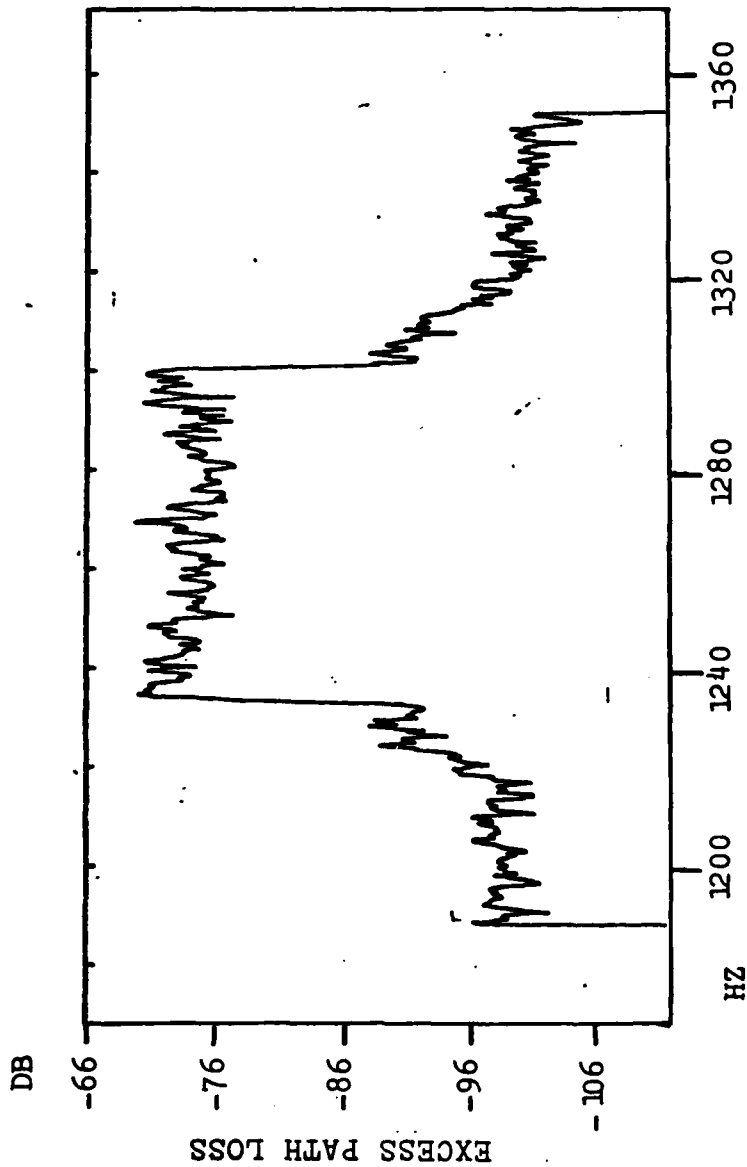


FIGURE 11. VERTICAL RECEIVED SPECTRUM

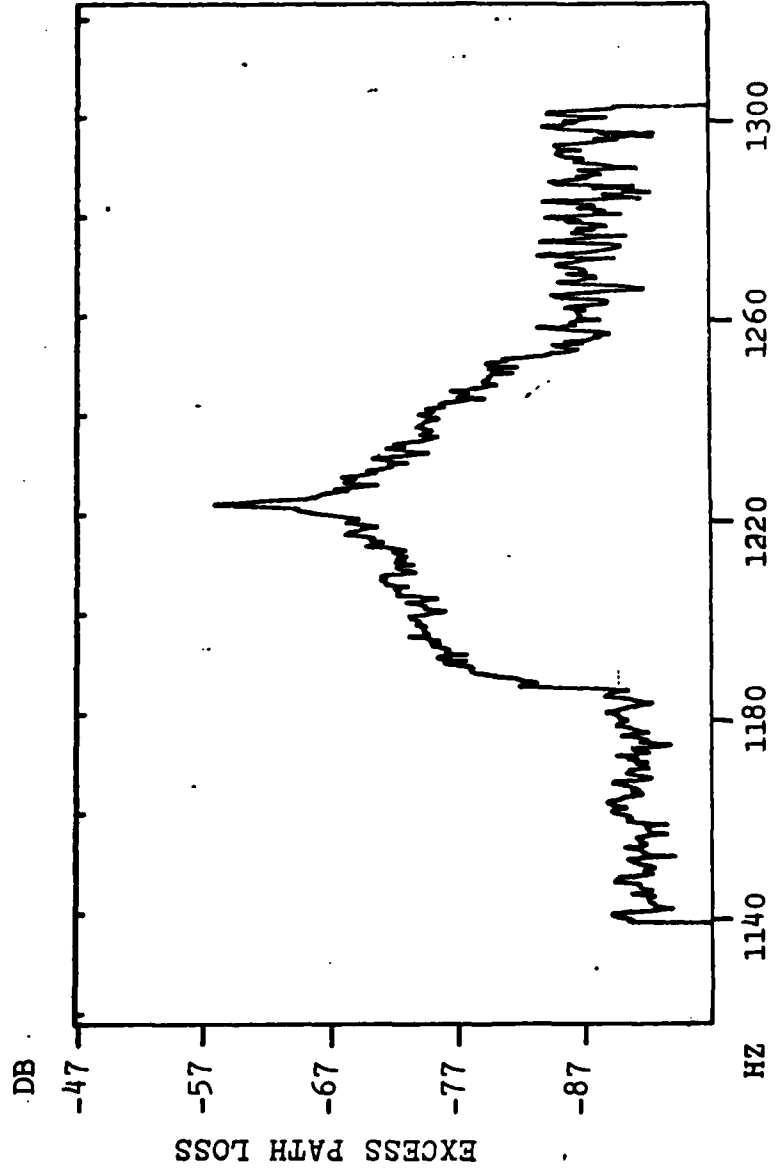


FIGURE 12. HORIZONTAL RECEIVED SPECTRUM

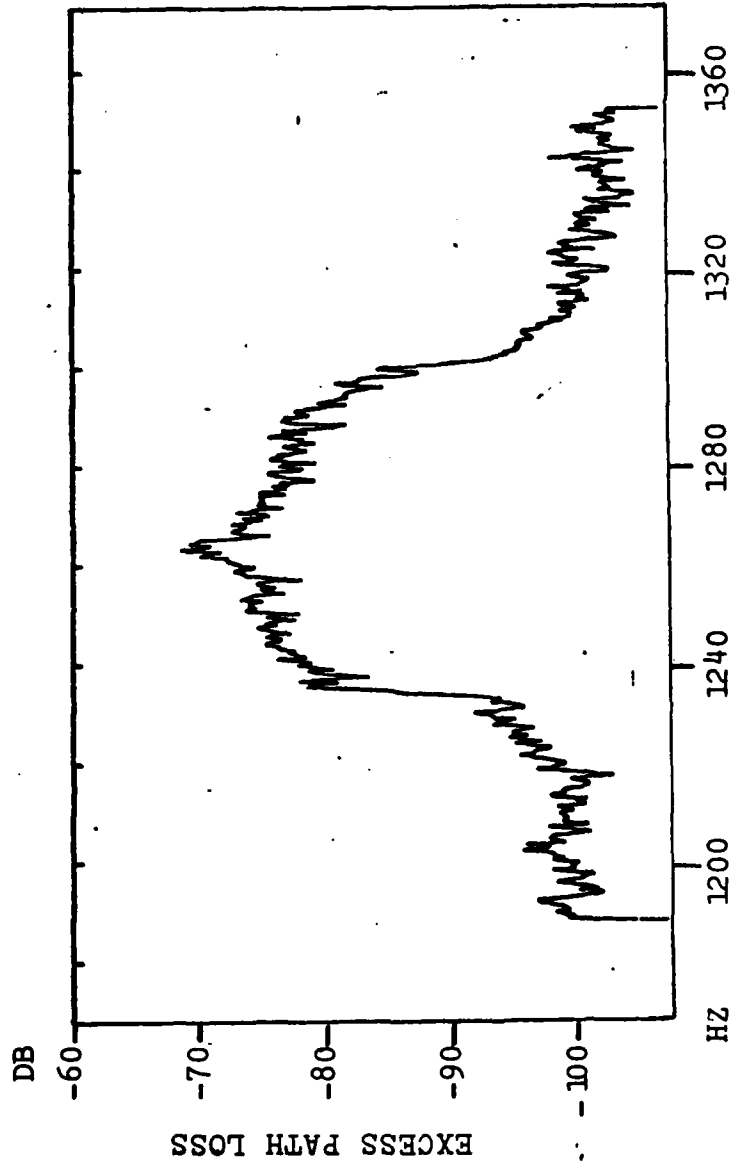
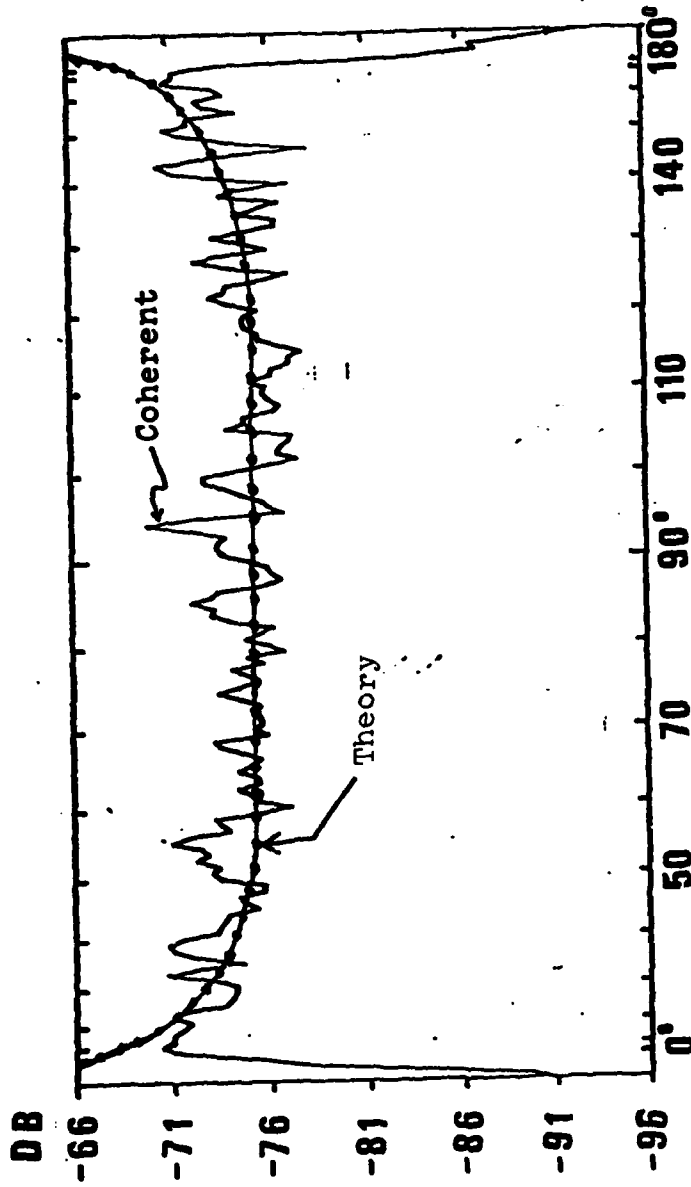


FIGURE 13. CROSS-POLARIZED RECEIVED SPECTRUM

all three plots (about 67.2 Hz wide yielding a vehicle speed of 84.50 kph). The coherent intensity peak is also readily discernible at the center frequency in each case.

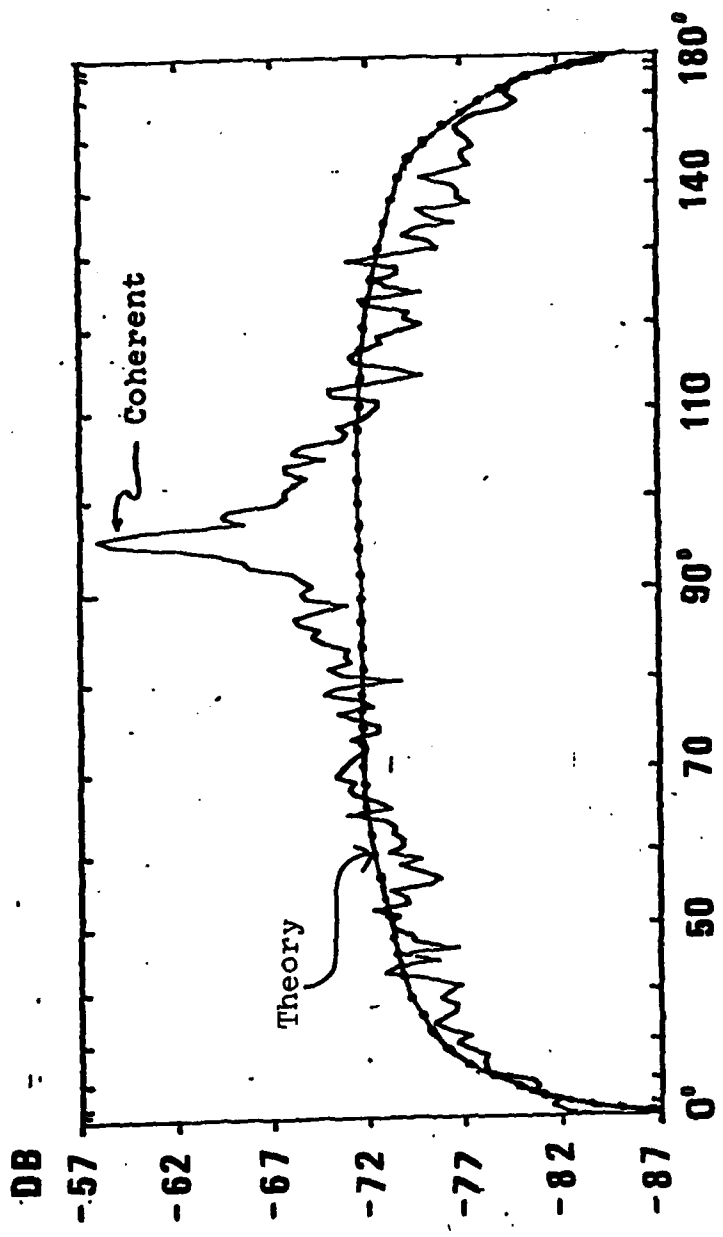
The free-space-loss (FSL) for the line-of-sight signal path in the experiment is 104 dB at 432 MHz. The dB scales of the plots, which show the excess path loss beyond FSL, were calibrated by carefully measuring the noise floor of the receiver, taking into account the Hanning window, and labeling the plots accordingly. The noise floor measurements, and hence the labeled plots, are accurate to  $\pm 1$  dB. The excess path loss is due to the effect of the propagating medium on the radio wave. The general downward slope of the PSD curve noticeable in the higher frequencies of the horizontal data plots is due to the tuning of the received signal too close to the upper edge of the SSB receiver's narrow pass-band.

Figs. 14 - 16 show only the Doppler-spread bandwidth portion of the previous figures with the horizontal axis relabeled using equation 16 to present the data as an angular spectrum. Superimposed on the plots for the co-polarized runs is the theoretical incoherent PSD calculated from eq. 17 (ie., without the direct wave contribution) using the directive gain of the dipole for each orientation [36].



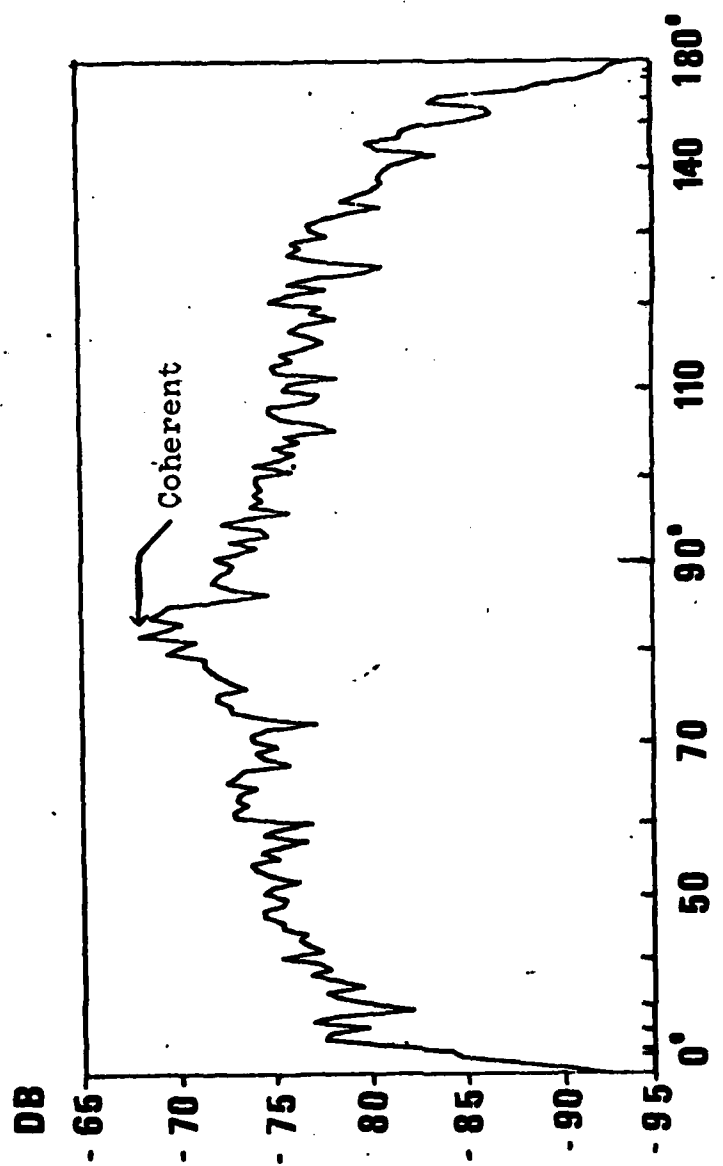
VERTICAL ANGULAR SPECTRUM

FIGURE 14



HORIZONTAL ANGULAR SPECTRUM

FIGURE 15



CROSS-POLARIZED ANGULAR SPECTRUM

FIGURE 16

Figs. 17 and 18 show the spatial autocorrelations of the incoherent intensity, in terms of number of wavelengths, for the co-polarized runs (see Appendix A for derivation of plots). The horizontal scale was determined via eq. 7 and the vertical scale denotes a normalized autocorrelation. The smooth curve indicated on the plots is the theoretical normalized autocorrelation plot based on the directive gain of the two antenna polarizations and the equation for the theoretical PSD (eq. 17) using a uniform  $p(\alpha)$  for incoherent intensity arrival angle.

#### DISCUSSION AND COMPARISON WITH PREVIOUS WORK

Figures 14 and 15 show the comparison of the measured PSD with the theoretical PSD of a uniform  $p(\alpha)$ . Such a  $p(\alpha)$  indicates that there is a uniform distribution of scattered energy incident on the receiving antenna over a 360 degree radius. Furthermore, this implies that the scattered wave amplitude is uncorrelated with the angle of arrival. If the forest can indeed be modeled using the uniform  $p(\alpha)$ , then a long transmission path can be represented at any point along the direction of travel of the mobile receiver as a uniform circle of equivalent scatterers centered on the antenna, despite the actual geometry of the environment.

In other words, scatterers that are at some depth in the forest stand are just as important in terms of received

# SPATIAL CORRELATION VERTICAL POLARIZATION

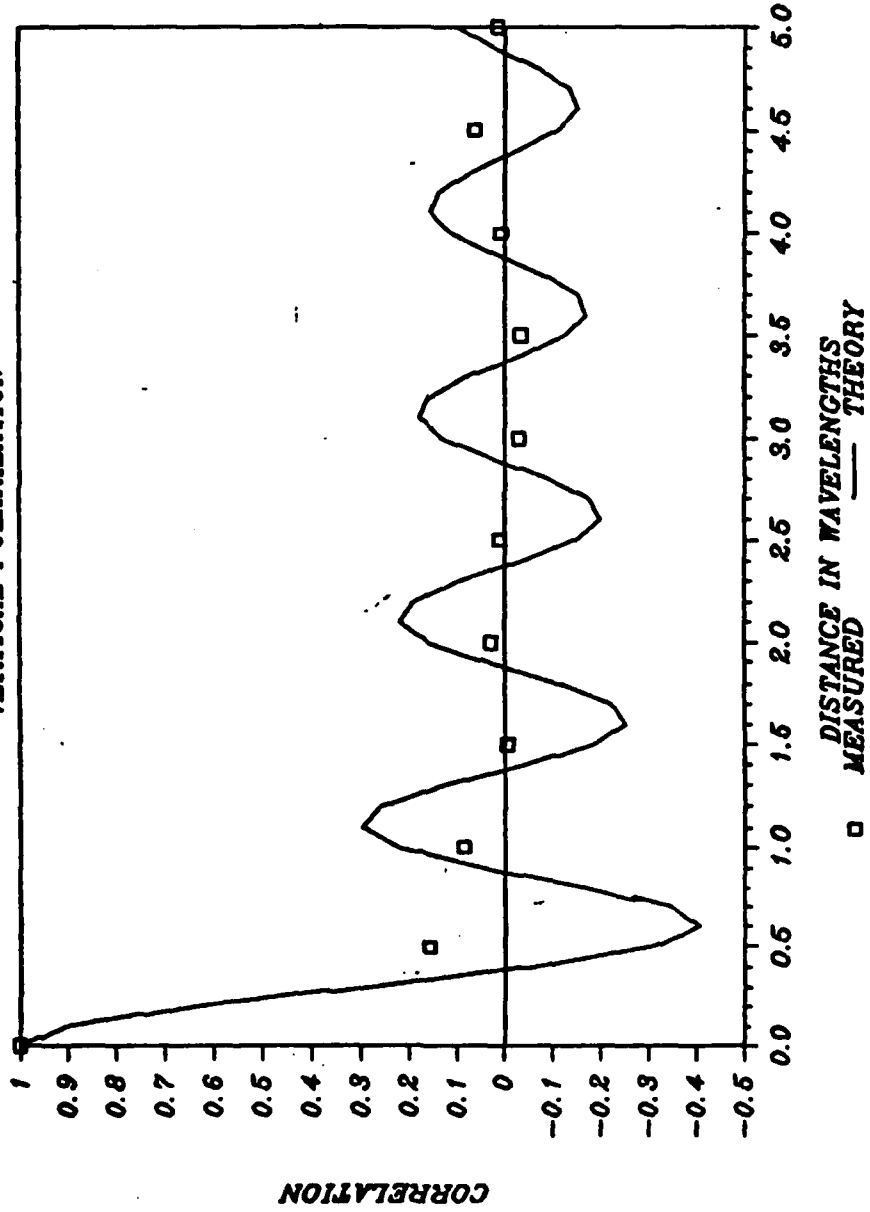


FIGURE 17

# SPATIAL CORRELATION HORIZONTAL POLARIZATION

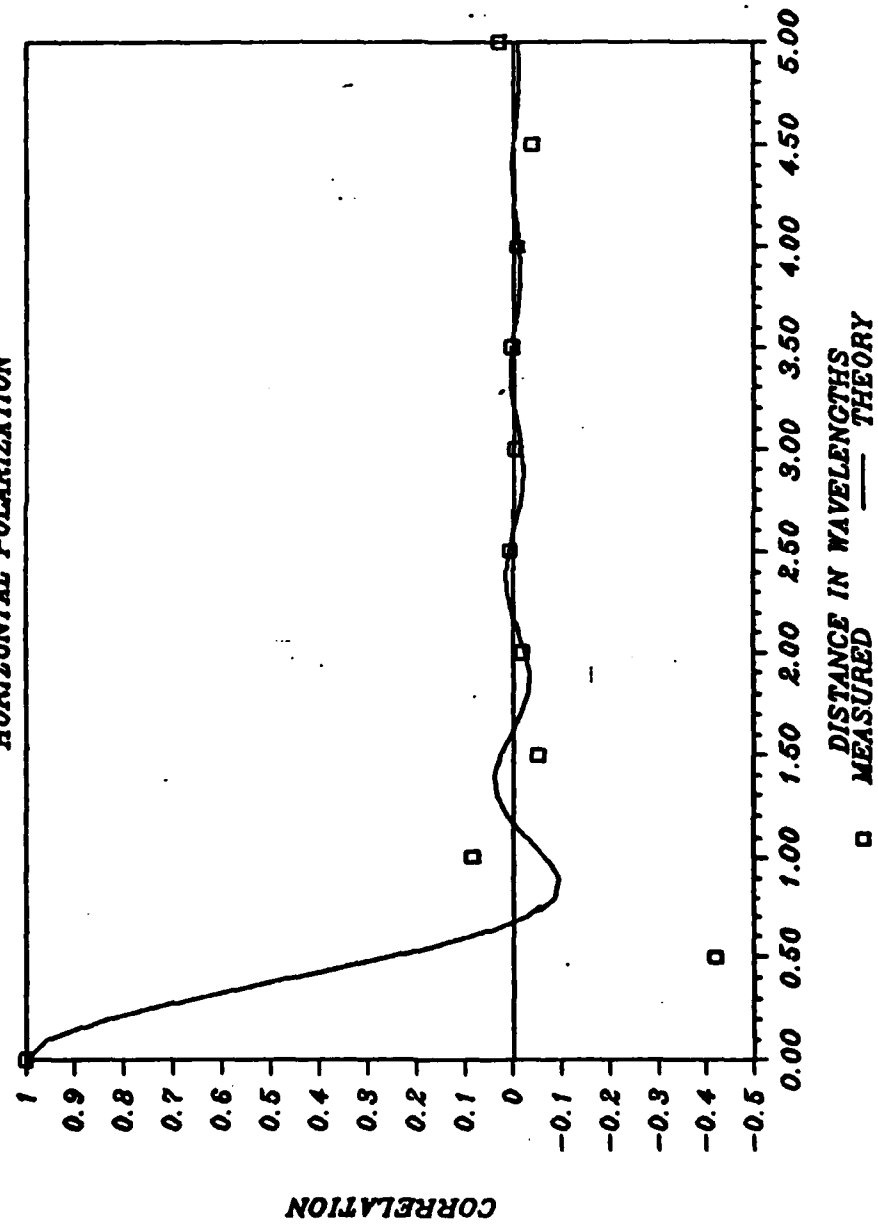


FIGURE 18

power as those adjacent to the road. Fig. 19 [18] shows the contrasting situation of a non-uniform  $p(\alpha)$  measured by Campbell in suburban Seattle, Wash. The fundamental difference between the two environments which may account for the distinct  $p(\alpha)$ 's is the more "fine-grained" nature of the forest: the trees are smaller and more numerous than are the buildings. This probably gives rise to higher-order multiple scattering effects [24] in foliage with the scattered intensity being uniformly diffused over all arrival angles as the wave propagates deeper into the forest. Hence, one must consider the effect on total intensity of trees deeper in the woods and not just those closest to the antenna.

Lang, et al. [5], have postulated that as the transmitted energy penetrates deeper into the forest, the incoherent field becomes progressively more important. This is evident from figs. 11-13. A measure of the ratio of coherent-to-total-intensity can be obtained from these figures by summing the values of the intensity within a few channels of the coherent peak and comparing it to the total intensity across the Doppler-spread bandwidth. Doing so yields a value of about 0.05 for the vertically co-polarized case, 0.42 for the horizontal case, and 0.21 for the cross-polarized situation (values accurate to about  $\pm 25\%$  of the stated value for each case). Data taken by Violette, et al, [6], indicates that for short transmission paths through a small number of trees, scatterers closest to

Frequency 432 MHz  
Signal Path - 1.57 KM  
Antenna - 0.10  $\lambda$  dipole  
Polarization - horizontal

... Theory with uniform p(a)  
--- Measured  
--- Theory with nonuniform p(a)  
(Reprinted from Campbell (18)  
with permission)

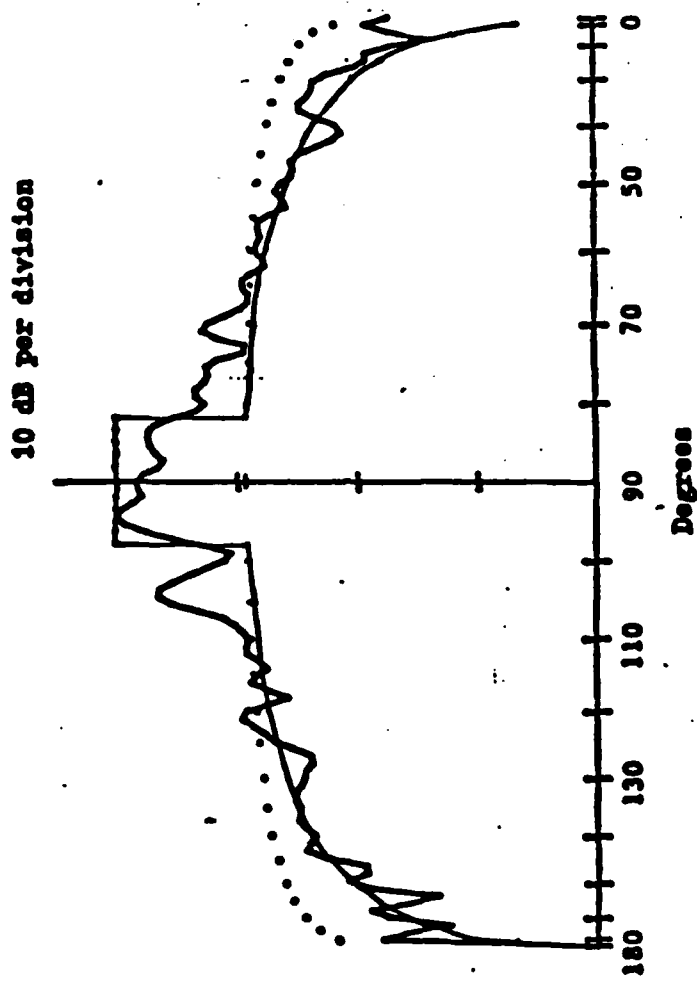


FIGURE 19. URBAN ENVIRONMENT COPOLARIZED ANGULAR SPECTRUM

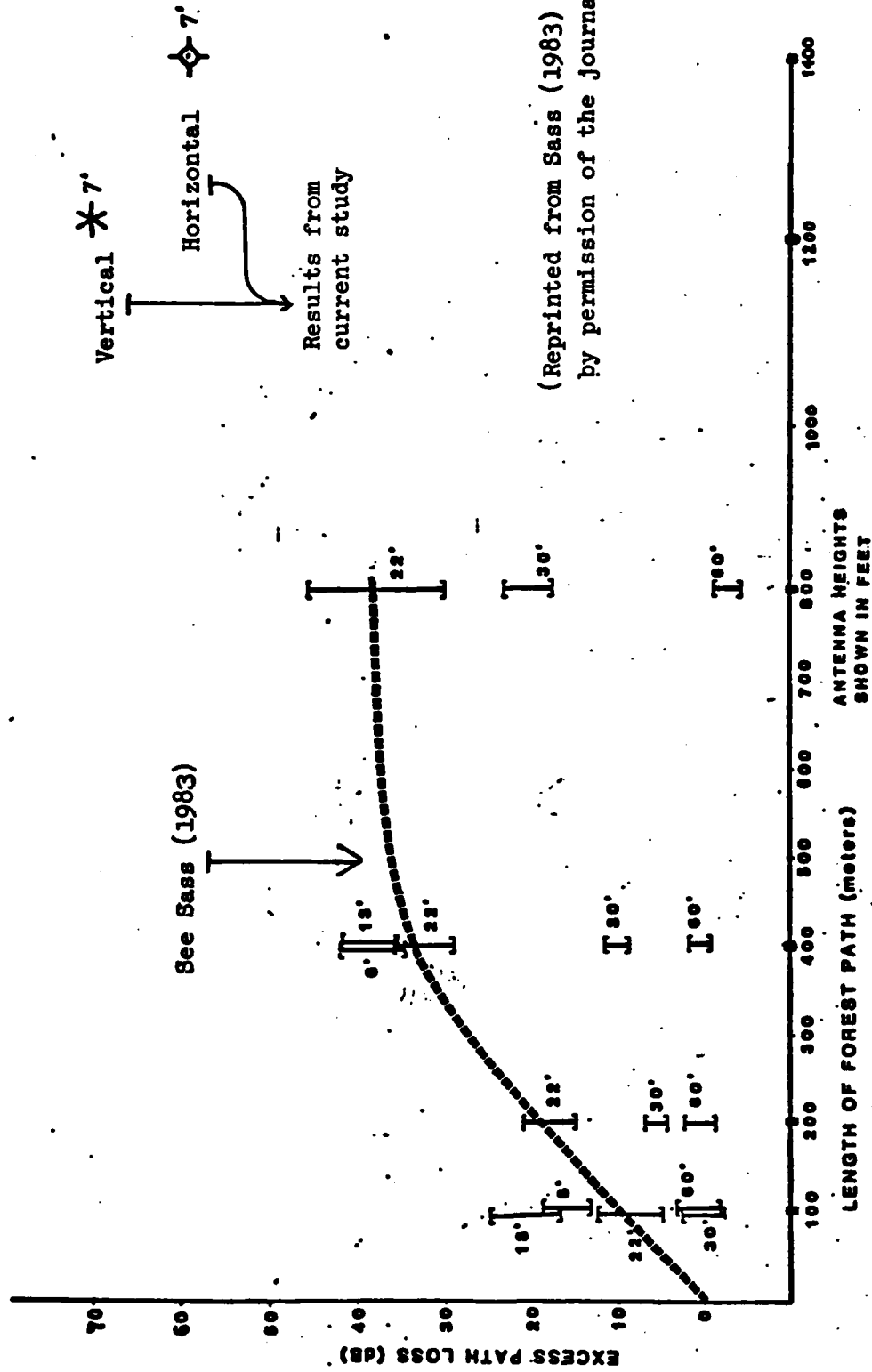
the receiver may dominate the received intensity as in the urban case (fewer, more discreet scatterers). The implication of the foregoing discussion is that the mode of propagation of the transmitted energy changes as the depth of penetration of the radiowave into the forest or foliage is increased. Indeed, the data suggest, as does Lang, et al [5], that as this depth increases, the coherent component of the intensity may be completely obscured (especially for the vertical co-polarized signal).

An important result of any propagation study is the observed basic transmission loss which is usually expressed in terms of an exponential "specific attenuation rate", " $\alpha$ " (in dB/m) (not to be confused with angle of arrival as used earlier). A number of both theoretical and empirical studies have attempted to examine and model the rate for propagation in a foliated environment (see references). Based on the received signal level of the coherent peaks of the PSD from figs. 11 and 12 and the average depth-of-foliage as seen by the receiver, the calculated " $\alpha$ " for the propagation path studied here is 0.06 dB/m for the vertically co-polarized case and 0.04 dB/m for the horizontal data. This is a somewhat simplistic representation of the complex attenuation process over the aggregate length of the signal path and presumes that all excess path loss is due to the foliage penetration experienced within 1.6 km of the

receiver (see fig. 9). The possible adverse effects of the coherent waves reflected from the surface of the lake (fig. 9), effects of the slight elevation change over the mobile receiver route, or from other sources of error are not considered.

The specific attenuation rates noted above are an order of magnitude lower than many of the measurements made by others in the same frequency range over shorter signal paths ([7], [8], and [23] ; Brown and Curry [3] and Sass [9] report results from multiple studies), but are consistent with the observation that the attenuation rate apparently decreases as depth of foliage penetration increases with the excess path loss generally following the pattern of fig. 20 [6,9]. This figure is from Sass [9] (by permission of the journal) and shows excess path loss as a function of antenna height from experimental tests of the US Army's "position locating and reporting system" (PLRS) in the frequency range 420-450 MHz. The results from the current study are plotted in the figure for comparison (polarization and forestation descriptions were not given by Sass). The actual curve for any specific situation will vary with geography, type of foliage, antenna heights, frequency, etc.

The ratio of the horizontal-to-vertical attenuation rate is in near agreement with the relationship at 432 MHz



(Reprinted from Sass (1983)  
by permission of the journal)

FIGURE 20. EXCESS PATH LOSS CURVE

hypothesized by the Rayleigh Effective Volume (REV) model for propagation in foliage developed by Brown and Curry (see Appendix D for a brief description of their model) [2,3] (see fig. D1 for the REV model as applied to a hypothetical forest). However, the magnitudes of the individual rates are smaller than would probably be predicted by REV for this study's environment as that model is only concerned with direct wave propagation and does not consider other lower-loss propagation modes that may arise over longer paths (as in fig. 20).

The usual explanation for the phenomenon described by fig. 20 has been [2] - [5] the lateral wave propagation theory developed initially by Tamir and extended by others [19] - [22]. The lateral wave theory of radio propagation through foliage models the forest as a dissipative dielectric slab or half-space, as characterized by some effective permittivity, lying on an imperfect conducting ground (the earth). Above the slab lies free space (see fig. 21). In the model the transmitted wave leaves the source antenna and some portion of it is refracted at the critical angle on the air-forest interface where it travels along the boundary in essentially free-space (lower-loss) conditions continually "leaking" energy back into the forest, some of which eventually reaches the receiver. This wave would be much less attenuated than the wave that travelled directly from

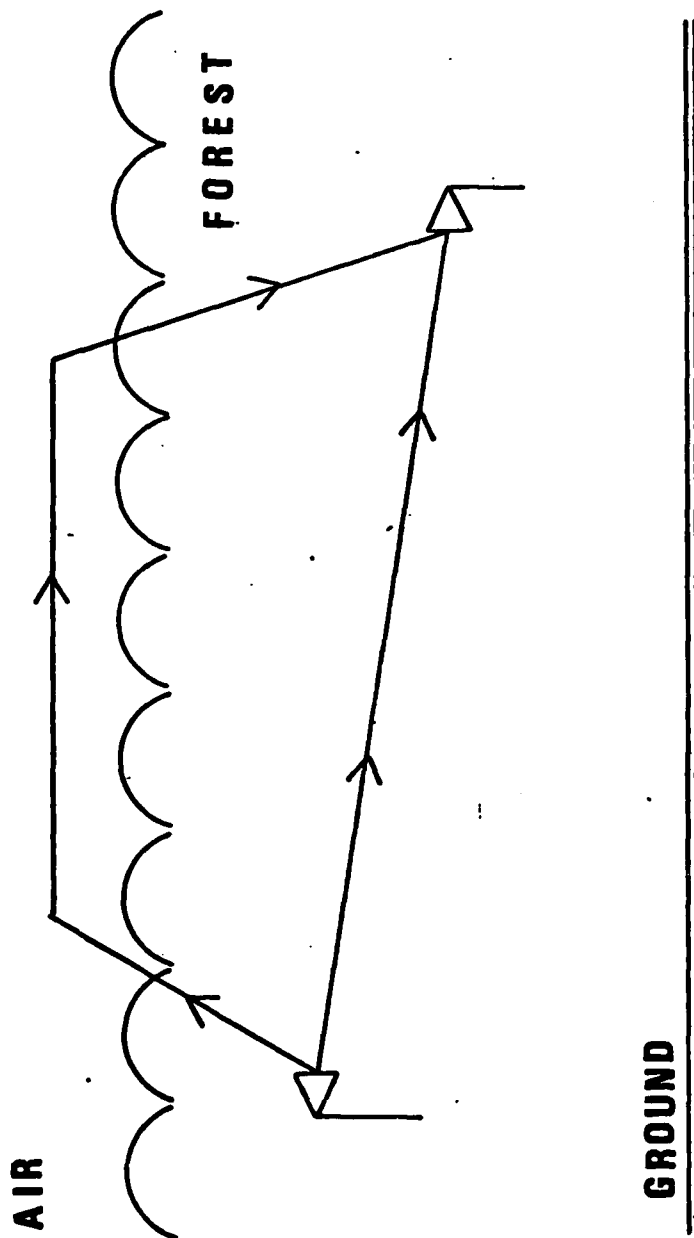


FIGURE 21. LATERAL WAVE MODEL

the transmitter through the slab (forest) to the receiver and, hence, should dominate the received field intensity on long paths. Tamir has shown [20] that the lateral wave may arise even if the transmitter is not immersed in the forest and/or more than one stand of forest (separated by free-space) occurs in the propagation path; both conditions which exist for the current study.

Despite its explanation of the nature of the excess path loss curve of fig. 20, recent studies reported by Violette [6] and Sass [9], which discuss measurements of parameters such as impulse response, multipath effects and propagation delays, in addition to basic transmission loss, suggest that the lateral wave may not be a wholly accurate representation of the propagation mechanism. They propose instead a "scattering mode of propagation". Although by no means conclusive, the results of this study also seem to support this contention. As noted above, one would expect the coherent intensity to dominate the received power spectrum given the lateral wave model. Also, if a lateral wave were present, then it seems reasonable, based on Violette's [6] observation regarding scattered intensity over short transmission paths noted above, that one might expect to see a definite correlation of intensity with arrival angle similar to the suburban study. This would arise from the relatively short path the lateral wave would travel from the

air-forest boundary back down to the receiver, but is apparently not the case in the results of this study.

In summary, then, the data presented here lend credence to the supposition that extended-range communications through forested areas is due to a "scatter propagation mechanism" rather than a lateral wave. In view of theoretical developments such as the REV model of Brown and Curry [2,3] and the work of Lang, et al [5], which show that scattering and absorption of radio waves are a function of the smaller (relative to about one-half wavelength or less) components of the forest bio-mass, it is conceivable that this mechanism could include a significant amount of energy being propagated by forward-scatter taking place in the upper regions of the forest canopy. More experimental studies of the power spectrum and the propagation parameters mentioned above are required for the development of a rigorous mathematical description of this proposed scatter propagation mode [9].

Figs. 13 and 16 are in agreement with the well-known observation that foliage causes a great amount of depolarization of the transmitted signal. The pattern of the cross-polarized PSD (receiver horizontally polarized) is consistent with a uniform probability of energy arrival

angle. The specific attenuation rate of 0.054 dB/m is slightly smaller than for the vertical-vertical case. This is expected from the results of the horizontally co-polarized data, the REV model of Brown and Curry [2,3], and other reports in the literature [5,6,19-21], which document significantly smaller attenuation in foliage of horizontally-polarized waves up to 0.5 - 1 GHz (above this frequency range, no appreciable difference is noticed or predicted). This is due to the vertical orientation and dielectric properties of the tree trunks [3,5] (see App. D). Further analysis of the cross-polarized data is hampered by the unknown effect of the small patch of trees at the transmitter site.

The spatial autocorrelation plots for the two-copolarized runs are presented in figs. 17 and 18 along with the Bessel function curves of the theory (see Appendix A). The pattern of the measured results show a general agreement with the theory given a uniform  $p(\alpha)$ . The vertical case appears to show a shift from the theoretical plot by a factor of 0.10 wavelengths. This suggests that the true receiver antenna pattern (as mounted on the vehicle) is not perfectly isotropic in the plane of reception (as the theoretical plot assumes). Deviation of the antenna pattern from an isotropic form will stretch the theoretical correlation curve along the horizontal axis and will dampen the

oscillations (the greater the deviation, the more pronounced the effects - see the plot for horizontal case). Additional factors that may help explain the deviation from the theoretical case for both polarizations are: 1) the environment is not perfectly stationary, and 2) the  $p(\alpha)$  is perhaps somewhat more complicated than the simple uniform expression discussed above (although the measurements do suggest that this is an adequate "simplification" for the purposes of modeling the propagation channel).

Lee [13] indicates an autocorrelation coefficient of 0.45 or less is required for the received fields to be uncorrelated. The measurements are in accordance with his observation that mobile radio signals are usually uncorrelated within a half of a wavelength. This has obvious advantages in the development of diversity/combining techniques to improve reception at the mobile receiver [10,13].

### CONCLUSIONS

The research presented here has been a successful attempt to verify the stochastic power-spectral-density theory of radio propagation as applied to a forested environment. Using a novel technique to achieve fractional-hertz resolution of the Doppler-spread received power spectrum, the resultant

data taken at 432 MHz over long transmission paths through the foliage shows reasonable agreement with the model as developed by Bell Labs, given a uniform probability distribution for the angle of arrival of incident energy on the receiving antenna. The data also provide a possible insight into the mode of propagation prevalent on the inter-foliage path. The results tend to support the contention of Hufford, et al [4], Violette, et al [6], and Sass [9] that the transition in propagation in this medium from a direct wave to a lower-loss mode over longer path lengths may be better characterized by a forward-scattering mechanism than by a lateral wave model. The measured ratios of coherent-to-total intensities reported here, which show a large amount of incoherent (scattered) intensity present in the received signal, together with the discovery of the uniform  $p(\alpha)$  for the intensity and the significant depolarization of the signal, suggest that high-order multiple-scattering theories (see [24]), such as the approach of Brown and Curry [2,3], may hold the key to accurate mathematical descriptions of the propagation phenomenon in this medium.

The results of this research have definite implications for the use of diversity techniques. The rapid decorrelation of the signal, as evidenced in figs. 17 and 18, suggests the use of space diversity to improve reception at mobile

receivers. The required antenna spacing of one - half - wavelength (evident from the spatial correlation plots) is certainly obtainable on most automotive platforms for frequencies in the upper VHF and UHF bands (see Lee [13] for information on combining technologies necessary to implement space diversity). As the receiver path will not always be oriented orthogonally to the transmitted signal as in this study, further research will be needed to determine the optimum placement of the antenna group on the vehicle.

The significant depolarization of the transmitted signal, as evidenced by figs. 13 and 16, suggests that the use of polarization multiplexing is not a viable means by which to achieve efficient use of limited frequency resources in applications requiring transmission through foliage.

Furthermore, the results of this study also confirm that horizontal polarization is the "polarization-of-choice" below 500 MHz in foliage (see Appx.D). The data gathered here suggests that horizontally polarized signals experience less excess path loss and retain a larger percentage of the signal in the coherent component than do vertically polarized signals over the same foliated transmission path.

It is recommended that the specific experiment described above be repeated over the same data paths at other times during the year to assess the effects of seasonal changes in

foliage. While the geography will not allow data to be compared from a multitude of signal paths at a variety of forest depths, the existence of an unimproved road just to the west of the road utilized in this study will provide a signal path that has about one-half of the foliage penetration reported here. It may also be instructive to gather data over both of these roads utilizing various antenna heights.

The specific techniques described in this thesis can certainly be utilized to study propagation in other locales and in different mediums. Further research at multiple frequencies of interest and over a number of paths varied in both type of foliage and depth of penetration are required to provide a definitive description and facilitate development of theoretical predictive models for UHF propagation in forests.

REFERENCES

- [1] US Army Field Manual (FM) 100-5 Operations, 1982.
  
- [2] Brown, G.S., and W.J. Curry, An analytical study of wave propagation through foliage, final report, contract F19628-78-C-0159, Appl. Sci. Assoc., Apex, N.C., 1980 (Available as "AD-A084348" from NTIS, see below).
  
- [3] Brown, G.S., and W.J. Curry, A theory and model for wave propagation through foliage, "Radio Science", 17(5), 1027-1036, 1982.
  
- [4] Hufford, G.A, R.W. Hubbard, et al, Wideband Propagation measurements in the presence of forests, final report, contract CS-1-CS029-CS-WA, US Dept. Commerce, NTIA/ITS, Boulder, CO, 1982 (available as "AD-A113698" from NTIS, see below).
  
- [5] Lang, R.H., A. Schneider, F.J. Altman, and Kiet Truong, UHF radiowave propagation through forests, annual report, contract DAAK80-81-C-0136, Cyber-Com Corp., Arlington, VA, 1984 (available as "AD-A149518" from NTIS, see below).

- [6] Violette, E.J., R.H. Espeland, and P. Schwering, Vegetation loss measurements at 9.6, 28.8 and 57.6 GHz through a pecan orchard in Texas, report number CECOM-83-2, US Dept. Commerce, NTIA/ITS, Boulder, CO, 1983 (available as "AD-A134149" from NTIS, see below).
- [7] Hunt, W.T., Propagation effects on satellite communication systems operating in the range of 240 to 3000 MHz, report number AFAL-TR-145, US Air Force Avionics Lab, Wright-Patterson AFB, OH, 1978 (available as "AD-A067535" from NTIS, see below).
- [8] Downey, M.J., Effects of trees and foliage on the propagation of UHF satellite signals, report number RSRE - 77017, Royal Signals and Radar Estab., Christchurch, U.K., 1977 (available as "AD-A048304" from NTIS see below).
- [9] Sass, P.F., Propagation measurements for UHF spread-spectrum mobile communications, "IEEE Trans. Veh. Technol.", VT-32(2), 168-176, 1983.
- [10] Jakes Jr., W.C., ed., Microwave Mobile Communications, 642 pp., Wiley-Interscience, New York, 1974.

- [11] Gans, M.J., A power-spectral theory of propagation in the mobile-radio environment, "IEEE Trans. Veh. Technol.", VT-21(1), 27-38, 1972.
- [12] Reudink, D.O., Properties of mobile radio propagation above 400 MHz, "IEEE Trans. Veh. Technol.", VT-23(4), 143-159, 1974.
- [13] Lee, W.C.Y., Mobile Communications Engineering, 464 pp., McGraw-Hill, New York, 1982.
- [14] Cox, D.C., Doppler spectrum measurements at 910 MHz over a suburban mobile radio path, "Proc. IEEE", 59 (6), 1017-1018, 1971.
- [15] -----, Delay Doppler characteristics of multipath propagation at 910 MHz in a suburban mobile radio environment, "IEEE Trans. Antennas Propag.", AP-20(5), 625-635, 1972.
- [16] -----, A measured delay-Doppler scattering function for multipath propagation at 910 MHz in an urban mobile radio environment, "Proc. IEEE", 61(4), 479-480, 1973.

- [17] Bullington, K., Radio propagation for vehicular communications, "IEEE Trans. Antennas Propag.", VT-26 (4), 295-308, 1977.
- [18] Campbell, R.L., Experimental studies of VHF and UHF propagation in an urban residential medium using high resolution RF spectral analysis, Ph.D. dissertation, 192 pp., Univ. of Washington, 1984 (available as No. 8501034, University Microfilms, Ann Arbor, MI 48109).
- [19] Tamir, T., On radio-wave propagation in forest environments, "IEEE Trans. Antennas Propag.", AP-15(6) 806-817, 1967
- [20] -----, Radio wave propagation along mixed paths in forest environments, "IEEE Trans. Antennas Propag.", AP-25(4), 471-477, ~~1967~~. 1977.
- [21] Dence, D., and T. Tamir, Radio loss of lateral waves in forest environments, "Radio Science", 4(2), 307-318 1969.

- [22] Cavalcante, G.P.S., D.A. Rogers, and A.J. Giarola, Radio loss in forests using a model with four layered media, "Radio Science", 18(5), 691-695, 1983.
- [23] Vogel, W.J., and E.K. Smith, Propagation considerations in land mobile satellite transmission, "Microwave Journal", 28(10), 111-130, Oct 1985.
- [24] Ishimaru, A., Wave Propagation and Scattering in Random Media, Vol.1&2, Academic Press, New York, 1978.
- [25] Whalen, A.D., Detection of Signals in Noise, 411 pp., Academic Press, New York, 1971.
- [26] Papoulis, A., Probability, Random Variables, and Stochastic Processes, 2nd Ed., 574 pp., Mc-Graw Hill, New York, 1984.
- [27] Ziemer, R.E., and R.L. Peterson, Digital Communications and Spread Spectrum Systems, 750 pp., Macmillan Publishing, New York, 1985.
- [28] Aulin, T., A modified model for the fading signal at a mobile radio channel, "IEEE Trans. Veh. Technol.", VT-28(3), 183-203. 1979.

- [29] Lee, W.C.Y., and R.H. Brandt, The elevation angle of a mobile radio signal arrival, "IEEE Trans. Veh. Technol.", VT-22(4), 110-113, 1973.
- [30] Cottam, G. and J.T. Curtis, A method for making rapid surveys of woodlands by means of pairs of randomly selected trees, "Ecology", 30(1), 101-104, 1949.
- [31] -----, Correction for various exclusion angles in the random pairs method, "Ecology", 36(4), 767, 1955.
- [32] Rice, F.L., and W.T. Penfound, An evaluation of the variable-radius and paired-tree methods in the blackjack-post oak forest, "Ecology", 36(2), 315-320, 1955.
- [33] HP 5451C System Operating Manual (w/ changes), Vol 1., Hewlett-Packard Corp., Fort Collins, CO, 1979 (available as HP part no. 05451-90529).
- [34] Bendat, J.S., and A.G. Piersol, Random Data Analysis and Measurement Procedures, 2nd Ed., 566 pp., Wiley-Interscience, New York, 1986.

- [35] Harris, F.J., On the use of windows for harmonic analysis with the discrete Fourier transform, "Proc. IEEE", 66(1), 51-83, 1978.
- [36] Balanis, C.A., Antenna Theory Analysis and Design, 790 pp., Harper and Row, New York, 1982.
- [37] Atkinson, K., Elementary Numerical Analysis, 416 pp., John Wiley and Sons, New York, 1985.

The address for the National Technical Information Service (NTIS) is listed below. Documents will be provided for a small fee. Military-affiliated users may obtain them directly from the Defense Technical Information Center (202-274-7633).

NTIS

5285 Port Royal Rd.

Springfield, VA 22161

## APPENDIX A: DERIVATION OF THEORETICAL PLOTS

### POWER SPECTRAL DENSITIES

The PSD plots of fig. 4a-c were obtained in the following manner. First, given a uniform  $p(\alpha)$  and an isotropic antenna (as in the vertical co-polarized case), the expression for the normalized PSD in eq. 17 simplifies to:

$$S(f) = 1/[1 - (\frac{f-f_c}{f_m})^2]^{1/2} \quad (A1)$$

This yields fig. 4a when plotted as an angular spectrum (using eq. 16) and presented in dB.

The power pattern in the elevation plane of a half-wave dipole is [36]:

$$[\cos^2(\frac{\pi}{2} - \cos\theta)] / \sin^2(\theta) \quad (A2)$$

For the antenna orientation in this experiment,  $\alpha = \theta$  (see fig. 7b). The plot of eq. A1 multiplied by eq. A2 results in fig. 4b, the plot for the horizontal polarization.

In the suburban study, Campbell [18] used a small dipole with the following pattern:

A2

$$G(\alpha) = \sin^2(\alpha) \quad (A3)$$

This results in the expression for the normalized PSD:

$$S(f) = \left[ 1 - \left( \frac{f - f_c}{f_m} \right)^2 \right]^{\frac{1}{2}} \quad (A4)$$

and plotted as an angular spectrum in fig. 4c.

#### THEORETICAL SPATIAL CORRELATIONS

The theoretical spatial correlations (of incoherent intensity only) were obtained as follows. Since the measured PSD is a real even function, its autocorrelation function is expressed [10]:

$$R_{uu}(t) = 2 \int_{f_c}^{f_c+f_m} S(f) \cos[2\pi(f - f_c)t] df \quad (A5)$$

Substituting in eq. A5 the expression for the PSD for the vertical case (eq. A1), and noting from eq. 16 that:

$$df = -f_m \sin(\alpha) d\alpha \quad (A6)$$

$$\sin(\alpha) = \left[ 1 - \left( \frac{f - f_c}{f_m} \right)^2 \right]^{\frac{1}{2}}$$

And simplifying the resultant equations while changing the limits of integration via eq. 16, results in an expression

for the normalized autocorrelation of the vertical copolarized case:

$$R_{uu}(t) = \frac{2}{\pi} \int_0^{\pi} \cos[2\pi f_m (\cos \alpha)t] d\alpha \quad (A7)$$

which is also a Bessel function of the first kind with order 0. To obtain the plot in fig. 17, eq. A7 was evaluated at various values of "t" utilizing a "BASIC" language computer program incorporating the "Simpson's Rule" algorithm of numerical analysis [37]. The results were accurate to at least 4 decimal places (as compared to published tables). The theoretical plot for the horizontal case (fig. 18) was done by the same program, however the integrand was eq. A7 multiplied by eq. A2 (antenna pattern with  $\theta = \alpha$ ). The temporal autocorrelation results obtained by the above process could be converted to spatial correlations via eq. 7 with the distance expressed in wavelengths.

#### MEASURED SPATIAL CORRELATIONS

In order to directly compare the measured data to the theoretical incoherent spatial correlations, it was necessary to remove the coherent component of the PSD and then take the inverse Fourier Transform to obtain a "processed" spatial correlation. Using the point-by-point channel fill capability of the HP 5451C, the few channels of

the coherent component portion of the 168-channel-wide Doppler-spread spectrum (the "peaks" of the PSD plots) were replaced in the data block with values similar to the adjacent non-coherent channels. The resultant data block was compared both visually and numerically with the original to insure a "proper" fit of the "massaged" data, i.e., a data-block that would have occurred if no coherent peak was present. This "processing" technique was used for each of the three polarization situations examined in the study.

The HP 5451C can only perform an inverse Fourier transform on the full-width 512 channel data block of figs. 11 - 13. To obtain a transform of the 168-channel Doppler-spread portion of the "processed" data-block, it was necessary to print out the channel values and transfer them by hand to a personal computer disk file for further calculation. A "BASIC" language program was written using the following equation to perform the inverse transform [33], [34]:

$$f(n \Delta t) = \sum_{m=0}^{167} P(m \Delta f) \cos (2 \pi n m / 168) \quad (A8)$$

This equation treats the data as having a data-block size of 168 while maintaining the 0.4 Hz spacing. Since the relationships between block-size  $N$ ,  $\Delta f$ ,  $\Delta t$ , and  $T$  (total length of the time record) are as follows [34]:

$$T = 1 / \Delta f \quad ; \quad \Delta t = T/N \quad (A9)$$

the resultant points of the autocorrelation function from eq. A8 are spaced at one-half-wavelength intervals and the plots can be labeled accordingly. The autocorrelation is normalized by dividing all values by  $R_{uu}(0)$ , which is the total power in the PSD (ie, integration of the PSD curve).

APPENDIX B: RANDOM-PAIRS METHOD OF FOREST SURVEY

The random-pairs method is a proven technique for making fairly rapid and accurate surveys of forest stands [30] - [32]. It is based on the premise that the number of trees per unit area can be calculated from the average distance between trees. If one considers the trees in a forest to occupy the centers of regular contiguous hexagons, then the mean area per tree (MA) is :

$$MA = (0.5 d)^2 * 3.4644 \quad (B1)$$

$$\text{or } MA = d^2 * 0.8661 = (0.93 d)^2$$

where "d" is the average distance between trees. Dividing MA into the unit area of interest yields the trees per unit area.

The field conduct of the survey method is not quite as easy as it first may seem. Simply taking trees at random in the woods and measuring the distance to their nearest neighbors will result in a density figure that is greater than the true figure. This results from measuring the distance between the two closest trees, not between trees that are an average distance apart.

To insure valid measurements, data on the trees are taken as shown in fig. B1. Sample points are picked in the woods by some method useful to the situation as determined by the surveyor. The technique used by the author was to take points 50 - 60 paces apart on East-West compass lines through the area of interest in fig. 8. A line is then drawn (by stretching a string) from the point to the closest tree. Another line perpendicular to the first is then placed through the sample point (as in fig. B1). This line then forms a 180 degree "exclusion angle" with its vertex at the sample point. Other exclusion angles such as 160 degrees may be used (so long as calculations are adjusted as noted below) but the 180 degree angle is easiest to use in the field. It is called the "exclusion angle" because all trees that fall inside of it may not be considered when looking for the next tree in the "random pair". This second tree of the pair is taken as the tree that lies closest to the line forming the exclusion angle but outside of the exclusion zone.

Initial comparison of the random-pairs technique using the formula in eq. B1 to more comprehensive forest surveying procedures showed that the former yielded biased estimates of MA [31]. It was found that the angle of exclusion corresponded to a specific correction factor in the calculation for the MA such that:

B3

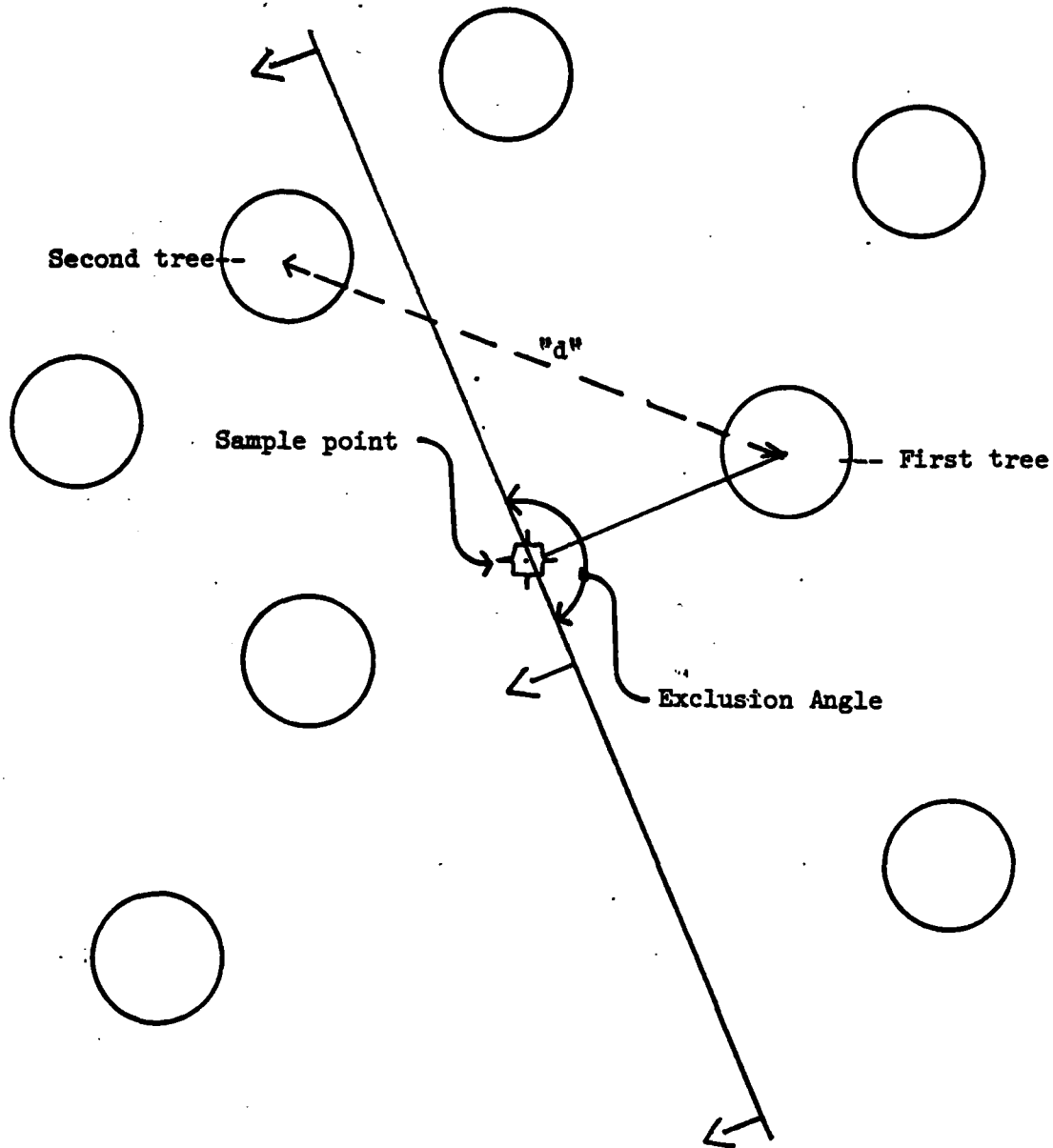


FIGURE B1. RANDOM-TREE-PAIRS SURVEY TECHNIQUE

$$\text{"True" MA} = (\text{C.F. times "d"})^2 \quad (\text{B2})$$

The correction factor (C.F.) for various angles of exclusion are as follows (180 degree angle was used in this research):

<u>ANGLE</u>	<u>C.F.</u>
0	1.67
30	1.43
100	1.03
140	0.89
160	0.83
180	0.80

In practice, this method is used to sample trees in the forest with diameters at breast height (DBH) of 4 or more inches. Trees smaller than this are considered as "reproduction - class" specimens and were surveyed in this report by taking the average amount found in a number of randomly-selected 2600-square-foot plots in the area-of-interest and translating that to a figure for average number per unit area (see table 1).

Tree heights were estimated using a "MERRITT" hypsometer. This is simply a trigonometrically-calibrated stick held vertically out from the surveyor's body at about three-quarters of an arms-length while he is standing a prescribed distance from the tree. The tree height is then read by noting where the top of the tree registers on the stick.



$$\begin{aligned}
 \text{Frequency increment} \quad \Delta f &= 1/T \\
 &= 2F_{\max}/N
 \end{aligned}
 \tag{C2}$$

The Fourier Analyzer uses the following equations to perform Fourier Transforms [33], [34]:

$$\begin{aligned}
 F(m \Delta f) &= (1/N) \sum_{n=0}^{N-1} f(n \Delta t) \exp(-j2\pi nm/N) \\
 f(n \Delta t) &= \sum_{m=0}^{N-1} F(m \Delta f) \exp(+j2\pi nm/N)
 \end{aligned}
 \tag{C3}$$

When taking an inverse transform (second equation), the analyzer assumes a symmetrical spectrum and therefore computes a pure real time series [33].

Processing a single time record (of length "T") results in an inconsistent estimate of the PSD (normalized standard error equals 1; see [34]). A consistent estimate can only be achieved by averaging a number of time records (see text). The number of averages available for processing the data of this study was limited by the total length of the individual data runs (see below).

Using the basic hardware configuration of the 5451C, the best frequency resolution we might obtain in this study was

1 Hz per channel (based on  $F_{max}$  of 2048). However, the Band-Selectable-Fourier-Analysis software present on the disk operating system allows greater channel resolution and concentration of processing about a selected band of frequencies within in the original sample record. This is obtained through a form of complex modulation where-by the sampled band-limited frequency records (as selected by the specific frequency band the user wishes to concentrate the processing on) are translated to base-band. This lowers the  $F_{max}$  in the record and allows increased frequency resolution [34].

The HP 5451C was set-up as follows to process the data for this report. The "TOTAL TIME" (length of a sample record) was set to 1 second on the ADC and only channel A was used. The BSFA program was called via key-board commands. Analog through-put block size was set to 4096. BSFA block size was set to 1024 (maximum available; yields 512 channels in the frequency domain). The number of time domain records that could be sampled were determined by the following equation (BS = blocksize).

$$\# \text{ Thru-put Records} = \text{Zoom Power} * \frac{\text{BSFA BS}}{\text{T-put BS}} * \# \text{ averages (C4)}$$

(of length set  
on ADC)

$$\text{Zoom Power} = F_{max}/(\text{band-width to be examined}) \quad (\text{C5})$$

The frequency band we wished to concentrate on was the 150 Hz-wide band centered on the  $\sim 1200$  Hz center frequency of the out-put of the drift-correction board (see fig. 5 and text). The closest the processor could come to our desired 150 Hz bandwidth was 204.8 Hz. This yielded a zoom power of ten, and limited the processing to either 16 or 22 averages in order to include data from the entire length of each data run (41.5 seconds total recording time for each vertical and cross-polarized run and 55 seconds for each probe and horizontal run - see text; more averages also decrease the standard normal error). This results in a  $\Delta f$  of 0.4 Hz for the BSPA processed data.

APPENDIX D: RAYLEIGH-EFFECTIVE-VOLUME MODEL [2], [3]

The following is a brief presentation of Brown and Curry's REV model of direct wave propagation in forests [2],[3]. The model is based on the observation that the woody components of a forest comprise less than 0.5% of the total volume (despite what one may intuitively think from just looking at a forest; a case of not being able to see the unoccupied-air-space for the trees!). This allowed Brown and Curry to use the Foldy-Twersky theory of wave propagation thru a sparse concentration of discreet random objects [24, vol.2]. Noting that attenuation and scattering of radio waves is associated with the smaller (relative to one-half wavelength) components of the forest, they developed a fairly simple algorithm to determine the effective fractional volume of wood ( $\rho V_p$ ) necessary for the equations of Foldy-Twersky (see [2]).

The basic equations of the REV model are as follows:

$$k = k_0 ( 1 + (\rho V_p) ( \epsilon_r - 1)(q)[1 - j0.1] ) \quad (D1)$$

$$\text{Im}(k) = -k_0 (\rho V_p)(q)[ \epsilon_r'' + ( \epsilon_r' - 1)/10 ] \quad (D2)$$

where:  $k$  - wave number in foliage

D2

$k_0$  - free space wavenumber

$\epsilon_r$  - complex permittivity

(  $\epsilon_r''$  - imaginary;  $\epsilon_r'$  - real )

$q$  - polarization factor

= 0.25 for vertical polarized waves < 500MHz

= 0.125 horizontal polarized waves < 500MHz

= 0.167 any polarization for freq > 500MHz

The difference in the factors for the polarizations results from the vertical orientation of the tree trunks, which dominate the constituents of ( $\rho V_p$ ) below 500 MHz. Above this frequency, most of the trunk material drops out of the effective volume. The branches and leaves become the major components but are much more randomly oriented.

The real part of the dielectric constant of wood is centered around a value of about 50 while the loss factor (imaginary part of the complex permittivity) varies as a function of frequency and season. Both are variable with tree type.

The plot of fig. D1 results from eq. D2 using a value of 50 for the real part of the permittivity and values for the loss factor as taken from fig. 2 of reference [3]. It is unknown what the effective value of the complex permittivity or the effective volume ( $\rho V_p$ ) are for the forested environment used in this study.

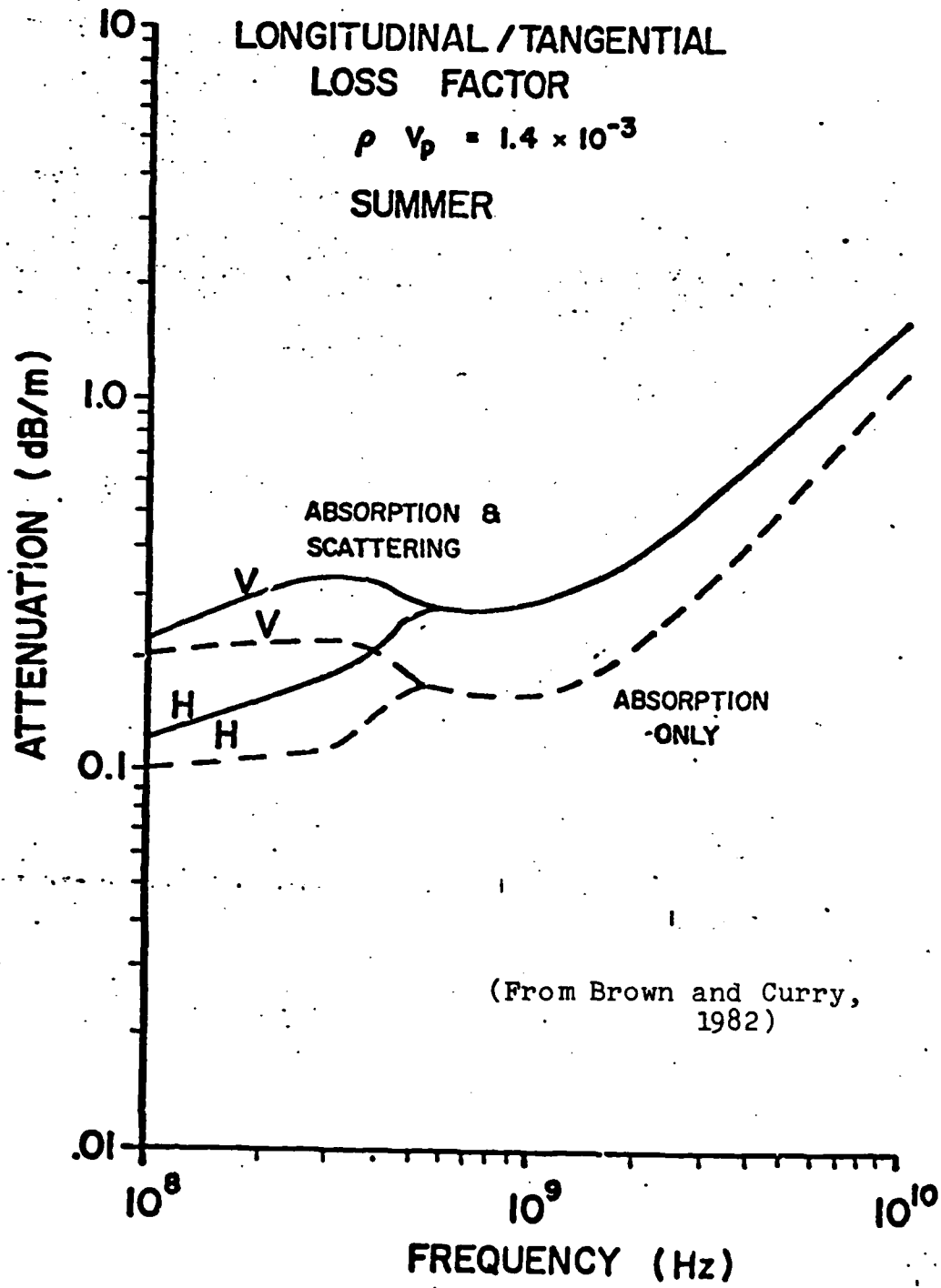


FIGURE D1. RAYLEIGH EFFECTIVE VOLUME  
PROPAGATION MODEL (REV)

D4

It should be reiterated that this model does not attempt to explain the low-loss propagation mode phenomenon of fig. 20, but rather is concerned only with the direct wave that propagates directly from the transmitter to the receiver (see fig. 21). Brown and Curry accept the lateral wave model to explain fig. 20.

AD-A171 431

INVESTIGATION OF THE UHF MOBILE-RADIO PROPAGATION  
CHANNEL IN A TEMPERATE-ZONE FORESTED ENVIRONMENT(U)  
ARMY MILITARY PERSONNEL CENTER ALEXANDRIA VA K J WHITE

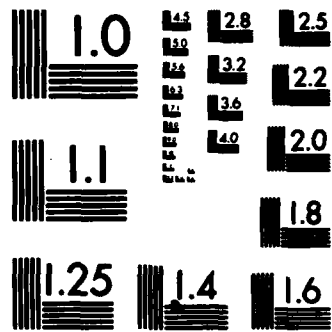
2/2

UNCLASSIFIED

13 AUG 86

F/G 17/2.1 NL





MICROCOPY RESOLUTION TEST CHART  
NATIONAL BUREAU OF STANDARDS-1963-A

## CURRICULUM VITAE

Kenneth James White was born 13 September 1956 in Kalamazoo, Michigan. He was graduated from Port Huron Northern High School, Port Huron, MI, in 1974. He studied forest and stream ecology and military science at The University of Michigan, Ann Arbor, MI, graduating in 1978 with a Bachelor of Science degree in Natural Resources (BSNR). In July of that year, he was commissioned as a Second Lieutenant in the US Army Signal Corps. After receiving training in combat communications at FT Gordon, GA and FT Sill, OK, LT White served for five years in the 8th (US) Infantry Division (Mechanized) in West Germany. His duty assignments included Communications Staff Officer for the division's Air Defense Artillery battalion, Intelligence Officer and later Operations Officer (S2/S3) for the 8th Signal Battalion, and commander of the signal battalion's Forward Communications Company. Upon his return to the states, CPT White attended the Dept. of Defense's senior communications school, the Telecommunications Systems Staff Officer Course at Keesler Air Force Base, MS. He was subsequently selected for advanced civilian schooling and attended Michigan Technological University in 1985-86 to pursue a Master's degree in Electrical Engineering. His follow-on duty assignment is with the Army Space Program, Los Angeles Field Office, LA Air Force Station. He and his wife Lynn are the proud parents of two sons, Leonard and Darren.

END

END

DTIC

9-86